

Estimating Factor-Based Spot Volatility Matrices with Noisy and Asynchronous High-Frequency Data

Degui Li*, Oliver Linton†, Haoxuan Zhang‡

University of York and University of Cambridge

This version: March 10, 2024

Abstract

We propose a new estimator of high-dimensional spot volatility matrices satisfying a low-rank plus sparse structure from noisy and asynchronous high-frequency data collected for an ultra-large number of assets. The noise processes are allowed to be temporally correlated, heteroskedastic, asymptotically vanishing and dependent on the efficient prices. We define a kernel-weighted pre-averaging method to jointly tackle the microstructure noise and asynchronicity issues, and we obtain uniformly consistent estimates for latent prices. We impose a continuous-time factor model with time-varying factor loadings on the price processes, and estimate the common factors and loadings via a local principal component analysis. Assuming a uniform sparsity condition on the idiosyncratic volatility structure, we combine the POET and kernel-smoothing techniques to estimate the spot volatility matrices for both the latent prices and idiosyncratic errors. Under some mild restrictions, the estimated spot volatility matrices are shown to be uniformly consistent under various matrix norms. We provide Monte-Carlo simulation and empirical studies to examine the numerical performance of the developed estimation methodology.

Keywords: continuous semimartingale, kernel smoothing, microstructure noise, PCA, spot volatility, time-varying factor models.

*Department of Mathematics, University of York, UK. Email: degui.li@york.ac.uk.

†Faculty of Economics, University of Cambridge, UK. Email: obl20@cam.ac.uk.

‡Department of Mathematics, University of York, UK. Email: hz885@york.ac.uk.

1 Introduction

In high-frequency financial econometrics, the so-called realised volatility has been commonly used to measure the integrated volatility of asset returns over a fixed time window (e.g., [Barndorff-Nielsen and Shephard, 2002, 2004](#); [Andersen *et al.*, 2003](#); [Shephard, 2005](#); [Aït-Sahalia and Jacod, 2014](#)). However, this results in a question of how to choose the time window, in particular when the financial market is volatile. In practice, it is often important to recover the actual spot/instantaneous volatility structure, which plays an important role in various applications such as testing price jumps (e.g., [Lee and Mykland, 2007](#)) and estimating stochastic volatility models (e.g., [Kanaya and Kristensen, 2016](#); [Bandi and Renò, 2018](#)). There have been many studies about spot volatility estimation. For the case of a single asset without market microstructure noise, [Fan and Wang \(2008\)](#) and [Kristensen \(2010\)](#) use a nonparametric kernel smoothing method to estimate the spot volatility function and derive its in-fill asymptotic properties. For the more general high-frequency data setting with microstructure noise, [Zu and Boswijk \(2014\)](#) propose a local version of the two-scale realised volatility ([Zhang, Mykland and Aït-Sahalia, 2005](#)) to estimate the spot volatility, whereas [Kanaya and Kristensen \(2016\)](#) combine classic kernel smoothing with the pre-averaging method ([Jacod *et al.*, 2009](#); [Christensen, Kinnebrock and Podolskij, 2010](#)).

Nowadays, practitioners often have to work with high-frequency financial data collected for a large number of assets. The aforementioned spot volatility estimation methods developed for a single or finite number of assets do not generally work well in the high-dimensional and high-frequency data setting. Under a uniform sparsity condition, [Bu *et al.* \(2023\)](#) estimate high-dimensional spot volatility matrices when the number of assets is ultra large, and derive the uniform convergence properties via the joint in-fill and increasing dimensionality asymptotics. However, the sparsity assumption imposed on large volatility matrices is too restrictive, since the price processes are often highly correlated between a large number of assets (in particular those from the same sector). It is well known that there may exist co-movements between these highly-correlated asset prices, and these co-movements may be captured by some latent risk factors. Hence, to relax the restrictive sparsity assumption and estimate meaningful volatility structures, the following continuous-time factor model is often employed for a p -dimensional vector of asset prices:

$$X_t = \Lambda F_t + U_t, \quad (1.1)$$

where Λ is a $p \times k$ matrix of constant factor loadings, F_t and U_t are k -dimensional and p -dimensional continuous semimartingales, respectively (see Section 2 for the definition). Model (1.1) is the approximate factor model, which has been extensively studied for low-frequency data (e.g., [Chamberlain and Rothschild, 1983](#); [Bai and Ng, 2002](#)). By imposing a sparse structural assumption on the volatility of U_t , it follows from (1.1) that X_t has a low-rank plus sparse volatility structure,

which is often called conditional sparsity (Fan, Liao and Mincheva, 2013). Fan, Furger and Xiu (2016) estimate the large (integrated) volatility matrix of X_t when the factors F_t are observable; whereas Aït-Sahalia and Xiu (2017) use the principal component analysis (PCA) to estimate the factor model (1.1) and further construct the large volatility matrix estimation for X_t when the factors are latent. Pelger (2019) estimates the factor model allowing jumps in the latent factor process and derives the convergence rates and limit distribution theory for the PCA estimated factors and loadings. Dai, Lu and Xiu (2019) estimate the conditionally sparse large covariance matrices and their inverse for the asynchronous high-frequency data which may be contaminated by the microstructure noise, combine the pre-averaging and generalised shrinkage in the estimation procedure and cover three different scenarios for the factor model specification. Other recent developments on estimation and testing of model (1.1) can be found in Kong and Liu (2018) and Sun and Xu (2022).

The continuous-time factor model (1.1) is essentially static with constant factor loadings. This model assumption may be insufficient when the main interest lies in the spot volatility matrix estimation. In particular, it becomes invalid when there are smooth structural changes or breaks in the process governing the large data series. This motivates the following time-varying factor model for continuous-time processes:

$$dX_t = \Lambda(t)dF_t + dU_t, \quad (1.2)$$

where $\Lambda(t)$ is a $p \times k$ matrix of time-varying factor loading processes and the other components are the same as those in (1.1). Model (1.2) covers model (1.1) as a special case when $\Lambda(t) = \Lambda$. It can be regarded as a natural extension of the time-varying factor model from the low-frequency data setting (e.g., Motta, Hafner and von Sachs, 2011; Su and Wang, 2017) to the high-frequency data setting. The aim of this paper is to estimate the large spot volatility matrix for X_t based on the time-varying factor model (1.2). Kong (2018) generalises Fan, Liao and Mincheva (2013)'s POET (Principal Orthogonal complement Thresholding) method to estimate the large spot volatility matrix of X_t defined in (1.2) and its decomposition into the systematic and idiosyncratic volatility components for noise-free and synchronised high-frequency data. In practice, it is not uncommon that the large high-frequency data are non-synchronised and may be contaminated by the market microstructure noise. A direct application of Kong (2018)'s method in the latter setting would result in biased volatility estimation. Hence, a substantial extension is required to address this problem and consistently estimate large spot volatility matrices. For the noisy high-frequency data but with observed (and possibly noise contaminated) factors, two recent papers by Bu *et al.* (2023) and Chen, Mykland and Zhang (2023) estimate the spot volatility structure of X_t under (1.2).

We assume the asset prices are observed with an additive noise structure to be defined in

Section 2.1, where the microstructure noise is allowed to be temporally correlated with nonlinear heteroskedasticity, asymptotically vanishing and dependent on the latent prices. The empirical studies in [Jacod, Li and Zheng \(2017\)](#) and [Li and Linton \(2022\)](#) reveal non-trivial temporal dependence for the microstructure noise of individual asset prices. The assumption of nonlinear heteroskedasticity allows the microstructure noise to have prominent intraday patterns such as the well-known U-shape. Some authors have argued that the microstructure noise is small in magnitude, and so, as in [Kalnina and Linton \(2008\)](#), we allow the microstructure noise to be shrinking as the data frequency increases. Such a “small noise” model structure is also adopted by [Da and Xiu \(2021\)](#) and [Li and Linton \(2023\)](#). Furthermore, we allow the noise to be correlated with the latent prices but do not impose any explicit correlation structure (e.g., [Kalnina and Linton, 2008](#)). The existence of endogenous noise may be due to rounding effects, price stickiness and asymmetric information (e.g., [Hansen and Lund, 2006](#)).

In practice different assets are traded at different frequencies and so their transaction prices are observed at times that are not synchronised and can be quite differently spaced due to liquidity levels varying over assets. This often leads to volatility matrix estimation bias and possibly enhances the so-called Epps effect (e.g., [Epps, 1979](#)). In order to jointly tackle the noise and asynchronicity issues, we extend the conventional pre-averaging method and introduce a kernel-weighted version, i.e., we take a weighted average of the observed prices over a local neighborhood of t by kernel smoothing to obtain an approximation of the latent price at time t . This kernel-weighted pre-averaging has been used by [Kanaya and Kristensen \(2016\)](#) in spot volatility estimation for a single asset, and recently has been adopted by [Bu et al. \(2023\)](#) in large spot volatility matrix estimation for synchronised high-frequency data. We show that the first-step kernel filter of the asset prices is uniformly consistent with the approximation order determined by the bandwidth, the dimension and the sample size, extending the uniform consistency derived by [Kanaya and Kristensen \(2016\)](#) and [Bu et al. \(2023\)](#) to a much more general setting.

To estimate the latent structure in the time-varying factor model (1.2), it is natural to apply a local version of PCA which relies on the local expansion of the smooth time-varying factor loading functions (e.g., [Motta, Hafner and von Sachs, 2011](#); [Su and Wang, 2017](#); [Kong, 2018](#); [Wang et al., 2021](#)). Since the latent prices are unavailable, we have to apply the local PCA to the estimated prices obtained via pre-averaging. This extension is non-trivial and leads to an extra challenge in proving the in-fill asymptotics for the local PCA estimates of common factors and factor loadings. The mean squared convergence rates for the estimated factors (taking the first-order difference) and the uniform convergence rates for the estimated time-varying factor loadings are slower than those in [Kong \(2018\)](#) who considers synchronised noise-free data. This is reasonable, since approximating latent prices results in extra estimation errors that consequently slow down the convergence rates for local PCA.

It follows from (1.2) that the spot volatility matrix of X_t is decomposed into the common and idiosyncratic spot volatility matrices. The latter is assumed to satisfy a uniform sparsity condition, which is similar to that used by [Chen, Xu and Wu \(2013\)](#), [Chen and Leng \(2016\)](#), [Chen, Li and Linton \(2019\)](#) and [Bu *et al.* \(2023\)](#), and results in the low-rank plus sparse matrix structure. Accordingly, we combine the classic POET with kernel smoothing to estimate the spot volatility matrices for both the latent prices and idiosyncratic errors. In particular, a generalised shrinkage technique is applied to the idiosyncratic spot volatility matrix estimation. We derive the uniform convergence property for the estimated idiosyncratic spot volatility matrix in the (elementwise) max and spectral norms, and obtain the rates comparable to those derived in [Chen, Mykland and Zhang \(2020\)](#) and [Bu *et al.* \(2023\)](#). Due to the spiked volatility structure, we derive the uniform convergence rates for the estimated spot volatility matrix of X_t not only in the max norm but also in the relative error measurement (e.g., [Fan, Liao and Mincheva, 2013](#); [Wang *et al.*, 2021](#)).

The finite-sample Monte-Carlo simulation studies show that the developed large spot volatility estimation method outperforms the naive estimation (without applying shrinkage to the estimated spot idiosyncratic volatility matrix). An empirical application to the one-min intraday log-price of S&P 500 index constituents reveals significant time-varying patterns of the spot volatility and covariance, and demonstrates rationality of the low-rank plus sparse spot volatility structure. In particular, the estimated factor number varies over time with fewer factors during the period of market collapse and more factors when the market is stable.

The rest of the paper is organised as follows. Section 2 introduces the additive microstructure noise model, low-rank plus sparse spot volatility matrix structure and estimation technique for large spot volatility matrices. Section 3 gives some regularity conditions and the in-fill asymptotic properties for the developed estimates together with some remarks. Section 4 conducts the Monte-Carlo simulation study and Section 5 reports the empirical application. Section 6 concludes the paper. Proofs of the main theoretical results and some technical lemmas are available in the Supplementary Material ([Li, Linton and Zhang, 2024](#)). Throughout the paper, we let $\|\cdot\|$ be the Euclidean norm of a vector; and for a $p \times p$ matrix $A = (A_{i_1 i_2})_{p \times p}$, we let $\|A\|_s$ and $\|A\|_F$ be the matrix spectral norm and Frobenius norm, $|A|_1 = \sum_{i_1=1}^p \sum_{i_2=1}^p |A_{i_1 i_2}|$, $\|A\|_1 = \max_{1 \leq i_2 \leq p} \sum_{i_1=1}^p |A_{i_1 i_2}|$, $\|A\|_{\infty, q} = \max_{1 \leq i_1 \leq p} \sum_{i_2=1}^p |A_{i_1 i_2}|^q$ and $\|A\|_{\max} = \max_{1 \leq i_1 \leq p} \max_{1 \leq i_2 \leq p} |A_{i_1 i_2}|$.

2 Model and methodology

In this section, we first introduce an additive noise structure for contaminated high-frequency data and the low-rank plus sparse spot volatility matrix structure, followed by description of the estimation methodology.

2.1 Microstructure noise

For the i -th asset, suppose that the asset prices are observed with the additive noise structure:

$$Y_{i,t_j^i} = X_{i,t_j^i} + \varepsilon_{i,t_j^i}, \quad i = 1, \dots, p, \quad j = 1, \dots, n_i, \quad (2.1)$$

where $X_{i,t}$ is the i -th component of X_t , $t_1^i, \dots, t_{n_i}^i$ are the data collection time points (which may be non-equidistant) for the i -th asset, and

$$\varepsilon_{i,t_j^i} = n_i^{-\beta_i} \chi_i(t_j^i) \varepsilon_{i,j}^*, \quad 0 \leq \beta_i < 1/2, \quad (2.2)$$

is the noise with $\chi_i(\cdot)$ and $\varepsilon_{i,j}^*$ satisfying Assumption 2 in Section 3.1 below. The general structure in (2.2) shows that the microstructure noise not only has a nonlinear heteroskedastic structure $\chi_i(\cdot)$, but also is asymptotically vanishing as the sampling frequency increases if $0 < \beta_i < 1/2$. In addition, we allow $\varepsilon_{i,j}^*$ to be correlated over i and j , and dependent on the latent prices X_{i,t_j^i} . Throughout the paper, we let $t_0^i \equiv 0$ and $t_{n_i}^i = T_i$.

The latent vector process $X_t = (X_{1,t}, \dots, X_{p,t})^\top$ satisfies the time-varying factor model structure (1.2), where F_t and U_t are k -dimensional and p -dimensional Brownian semimartingales, respectively, solving

$$dF_t = \mu_t^F dt + \sigma_t^F dW_t^F \quad (2.3)$$

and

$$dU_t = \mu_t^U dt + \sigma_t^U dW_t^U, \quad (2.4)$$

μ_t^F and μ_t^U are vectors of drift with dimensions k and p , respectively, σ_t^F and σ_t^U are $k \times k$ and $p \times p$ matrices of spot volatilities, W_t^F and W_t^U are k -dimensional and p -dimensional standard Brownian motions. The drifts and spot volatilities are progressively measurable processes. As in Kong (2018) and Pelger (2019), we assume that $\{W_t^F : t \geq 0\}$ and $\{W_t^U : t \geq 0\}$ are independent standard Brownian motions. This assumption may be relaxed to allow for weak correlation between the factor and idiosyncratic error processes. Without loss of generality, we may further assume that $\sigma_t^F = I_k$, a $k \times k$ identity matrix; otherwise, we can re-define the factor loading matrix as $\Lambda(t)\sigma_t^F$ in (1.2) and the drift as $(\sigma_t^F)^{-1}\mu_t^F$ in (2.3).

2.2 Large spot volatility matrices with conditional sparsity

Our main interest lies in estimating the factor-based spot volatility structure of the latent process X_t . For $0 < \tau < T$ with T being fixed, we let $\Sigma_X(\tau)$, $\Sigma_F(\tau)$ and $\Sigma_U(\tau)$ denote the spot volatility matrices for X_t , F_t and U_t , respectively. From (1.2), (2.3) and (2.4), assuming F_t and U_t are independent, we

readily have that

$$\Sigma_X(\tau) = \Lambda(\tau)\Lambda(\tau)^\top + \sigma_\tau^u (\sigma_\tau^u)^\top = \Sigma_C(\tau) + \Sigma_U(\tau), \quad (2.5)$$

indicating that $\Sigma_X(\tau)$ can be decomposed into the common and idiosyncratic spot volatility matrices: $\Sigma_C(\tau)$ and $\Sigma_U(\tau)$. Throughout the paper, we assume the following uniform sparsity condition: $\{\Sigma_U(t) : 0 \leq t \leq T\} \in \mathcal{S}(q, \omega_p)$ which is defined by

$$\left\{ \Sigma(t) = [\sigma_{i_1 i_2}(t)]_{p \times p}, t \in [0, T] \mid \Sigma(t) \succ 0, \sup_{0 \leq t \leq T} \|\Sigma(t)\|_{\infty, q} \leq \Psi \cdot \omega_p \right\}, \quad (2.6)$$

where “ $\succ 0$ ” denotes positive definiteness, $0 \leq q < 1$ and Ψ is a positive random variable satisfying $E(\Psi) \leq C_\Psi < \infty$. This is similar to the sparsity assumption used by [Chen, Xu and Wu \(2013\)](#), [Chen and Leng \(2016\)](#), [Chen, Li and Linton \(2019\)](#) and [Bu *et al.* \(2023\)](#) and is a natural extension of the approximate sparsity (e.g., [Bickel and Levina, 2008](#)).

With the sparsity restriction on $\Sigma_U(\cdot)$, we obtain a low-rank plus sparse (or conditionally sparse) structure on $\Sigma_X(\cdot)$. In the low-frequency data setting, [Fan, Liao and Mincheva \(2013\)](#) introduce the POET method to estimate the large covariance matrix of X_t which satisfies the discrete-time approximate factor model; and [Wang *et al.* \(2021\)](#) propose a local POET via kernel smoothing to estimate the large dynamic covariance matrix of X_t which satisfies the state-varying or time-varying factor model. Extending their methods to estimate $\Sigma_X(\cdot)$ is non-trivial since X_t is latent and $Y_{i,t}$ is non-synchronised. [Kong \(2018\)](#) generalises the POET method to estimate the spot volatilities $\Sigma_X(\cdot)$, $\Sigma_C(\cdot)$ and $\Sigma_U(\cdot)$ as well as their integrated versions for noise-free and synchronised high-frequency data. His method is not applicable to our high-frequency data setting and would result in biased volatility estimation due to presence of the microstructure noise and asynchronicity in model (2.1).

2.3 Estimation of the large spot volatility matrix

Partly motivated by [Kanaya and Kristensen \(2016\)](#) and [Bu *et al.* \(2023\)](#), we next introduce a kernel-weighted pre-averaging method to jointly tackle the microstructure noise and asynchronicity issues. The proposed technique is a local extension of the conventional pre-averaging which is introduced by [Jacod *et al.* \(2009\)](#) and [Christensen, Kinnebrock and Podolskij \(2010\)](#) to estimate the integrated volatility for a single asset and has been further extended by [Kim, Wang and Zou \(2016\)](#) and [Dai, Lu and Xiu \(2019\)](#) to estimate large matrices of integrated volatility.

Start with locally averaging the high-frequency observations Y_{i,t_j^i} via a kernel filter:

$$\tilde{X}_{i,t} = \sum_{j=1}^{n_i} (t_j^i - t_{j-1}^i) L_b(t_j^i - t) Y_{i,t_j^i}, \quad i = 1, \dots, p, \quad (2.7)$$

where $L(\cdot)$ is a kernel function, b is a bandwidth and $L_b(\cdot) = b^{-1}L(\cdot/b)$. The $\tilde{X}_{i,t}$ can be seen as a fitted value for the latent $X_{i,t}$, and Proposition 3.1 in Section 3.2 below establishes the uniform consistency property for $\tilde{X}_{i,t}$. We adopt the modified kernel weights $(t_j^i - t_{j-1}^i)L_b(t_j^i - t)$ in (2.7) to address the issue of irregular/asynchronous sampling times. For the special case of equally-spaced time points in high-frequency data collection, i.e., $t_j^i - t_{j-1}^i \equiv \Delta$, $j = 1, \dots, n_i$, the kernel filter in (2.7) can be simplified to

$$\tilde{X}_{i,t} = \Delta \sum_{j=1}^{n_i} L_b(t_j^i - t) Y_{i,t_j^i},$$

see Kanaya and Kristensen (2016).

Let $\tilde{X}_t = (\tilde{X}_{1,t}, \dots, \tilde{X}_{p,t})^\top$ and $t_j = j\Delta_o$, $j = 0, 1, \dots, N$, with Δ_o being a user-specified time difference and $N = \lfloor T/\Delta_o \rfloor$. We construct the kernel-weighted realised volatility matrix:

$$\tilde{\Sigma}_X(\tau) = \sum_{j=1}^N K_h(t_j - \tau) \Delta \tilde{X}_j \Delta \tilde{X}_j^\top, \quad (2.8)$$

where

$$\Delta \tilde{X}_j = \tilde{X}_{t_j} - \tilde{X}_{t_{j-1}} = \left(\Delta \tilde{X}_{1,j}, \dots, \Delta \tilde{X}_{p,j} \right)^\top.$$

With eigen-analysis on $\tilde{\Sigma}_X(\tau)$, we obtain $(\tilde{\lambda}_l(\tau), \tilde{\eta}_l(\tau))$, $l = 1, \dots, p$, as pairs of eigenvalues and normalised eigenvectors, where the eigenvalues are arranged in a descending order. From the matrix spectral decomposition, assuming the factor number is known a priori, we re-write

$$\tilde{\Sigma}_X(\tau) = \sum_{l=1}^k \tilde{\lambda}_l(\tau) \tilde{\eta}_l(\tau) \tilde{\eta}_l(\tau)^\top + \sum_{l=k+1}^p \tilde{\lambda}_l(\tau) \tilde{\eta}_l(\tau) \tilde{\eta}_l(\tau)^\top =: \tilde{\Sigma}_C(\tau) + \tilde{\Sigma}_U(\tau), \quad (2.9)$$

where $\tilde{\Sigma}_C(\tau)$ and $\tilde{\Sigma}_U(\tau)$ are the estimated spot volatility matrices at time τ for the common and idiosyncratic error components, respectively. By the construction in (2.9), $\tilde{\Sigma}_C(\tau)$ is a low-rank covariance matrix. With the sparsity restriction on $\Sigma_U(\cdot)$, we may further apply a generalised shrinkage. Let $s_\rho(\cdot)$ be a shrinkage function satisfying that (i) $|s_\rho(u)| \leq |u|$ for $u \in \mathcal{R}$; (ii) $s_\rho(u) = 0$ if $|u| \leq \rho$; and (iii) $|s_\rho(u) - u| \leq \rho$, where ρ is a user-specified tuning parameter controlling the level of shrinkage. Letting $\tilde{\sigma}_{u,i_1 i_2}(\tau)$ be the (i_1, i_2) -entry of $\tilde{\Sigma}_U(\tau)$, we define

$$\bar{\Sigma}_U(\tau) = [\bar{\sigma}_{u,i_1 i_2}(\tau)]_{p \times p} \quad \text{with} \quad \bar{\sigma}_{u,i_1 i_2}(\tau) = s_{\rho(\tau)}(\tilde{\sigma}_{u,i_1 i_2}(\tau)), \quad (2.10)$$

where $\rho(\cdot)$ is a time-varying tuning parameter. Consequently, we obtain the kernel POET estimate of $\Sigma_X(\tau)$:

$$\bar{\Sigma}_X(\tau) = \tilde{\Sigma}_C(\tau) + \bar{\Sigma}_U(\tau). \quad (2.11)$$

It follows from Theorem 1 in [Fan, Liao and Mincheva \(2013\)](#) and Proposition 1 in [Wang et al. \(2021\)](#) that the kernel POET estimate defined in (2.11) is equivalent to the local PCA method to be introduced shortly. By (1.2) with some smoothness condition on $\Lambda(\cdot)$ (see Assumption 1(iii) in Section 3.1), we may obtain the following local approximation of the time-varying factor model using the increments of the stochastic processes:

$$\Delta X_j K_h^{1/2}(t_j - \tau) \approx \Lambda(\tau) \Delta F_j K_h^{1/2}(t_j - \tau) + \Delta U_j K_h^{1/2}(t_j - \tau), \quad (2.12)$$

where $\Delta X_j = X_{t_j} - X_{t_{j-1}} = (\Delta X_{1,j}, \dots, \Delta X_{p,j})^\top$, ΔF_j and ΔU_j are defined analogously. As in (2.8), we replace ΔX_j by $\tilde{\Delta X}_j$ in the following local PCA. Write $\Lambda(\tau) = [\Lambda_1(\tau), \dots, \Lambda_p(\tau)]^\top$ with $\Lambda_i(\tau) = [\Lambda_{i,1}(\tau), \dots, \Lambda_{i,k}(\tau)]^\top$,

$$\begin{aligned} \tilde{\Delta X}(\tau) &= \left[\tilde{\Delta X}_1 K_h^{1/2}(t_1 - \tau), \dots, \tilde{\Delta X}_N K_h^{1/2}(t_N - \tau) \right], \\ \Delta F(\tau) &= \left[\Delta F_1 K_h^{1/2}(t_1 - \tau), \dots, \Delta F_N K_h^{1/2}(t_N - \tau) \right]^\top. \end{aligned}$$

Define the kernel-weighted least squares objective function:

$$\sum_{j=1}^N \left(\tilde{\Delta X}_j - \bar{\Lambda} \cdot \bar{F}_j \right)^\top \left(\tilde{\Delta X}_j - \bar{\Lambda} \cdot \bar{F}_j \right) K_h(t_j - \tau) = \left\| \tilde{\Delta X}(\tau) - \bar{\Lambda} \cdot \bar{F}(\tau) \right\|_F^2, \quad (2.13)$$

where $\bar{\Lambda}$ and \bar{F}_j are generic notation for the factor loading matrix and common factor in the local PCA estimation procedure, and $\bar{F}(\tau)$ is defined similarly to $\Delta F(\tau)$ but with ΔF_j replaced by \bar{F}_j .

Consider the following identification condition:

$$\Delta F(\tau)^\top \Delta F(\tau) = I_k \quad \text{and} \quad \frac{1}{p} \Lambda(\tau)^\top \Lambda(\tau) \text{ is diagonal}, \quad (2.14)$$

which are commonly used in PCA estimation of the factor models (e.g., [Bai and Ng, 2002](#); [Fan, Liao and Mincheva, 2013](#); [Chen, Mykland and Zhang, 2020](#)). With the identification condition (2.14), we replace $\bar{\Lambda}$ in (2.13) by $\tilde{\Delta X}(\tau) \bar{F}(\tau)$. Then, the kernel-weighted objective function in (2.13) becomes

$$\text{trace} \left\{ \tilde{\Delta X}(\tau)^\top \tilde{\Delta X}(\tau) \right\} - \text{trace} \left\{ \bar{F}(\tau)^\top \tilde{\Delta X}(\tau)^\top \tilde{\Delta X}(\tau) \bar{F}(\tau) \right\},$$

indicating that minimising (2.13) subject to the restriction (2.14) is equivalent to maximising the trace of $\bar{F}(\tau)^\top \tilde{\Delta X}(\tau)^\top \tilde{\Delta X}(\tau) \bar{F}(\tau)$ subject to $\bar{F}(\tau)^\top \bar{F}(\tau) = I_k$. Hence, we conduct the eigen-analysis on the $N \times N$ matrix $\tilde{\Delta X}(\tau)^\top \tilde{\Delta X}(\tau)$ and obtain the local PCA estimate of $\Delta F(\tau)$:

$$\tilde{\Delta F}(\tau) = \left[\tilde{\Delta F}_1(\tau), \dots, \tilde{\Delta F}_N(\tau) \right]^\top$$

which is a matrix consisting of the eigenvectors corresponding to the k largest eigenvalues. Furthermore, the time-varying factor loading matrix $\Lambda(\tau)$ is estimated as

$$\tilde{\Lambda}(\tau) = \Delta \tilde{X}(\tau) \Delta \tilde{F}(\tau) = \left[\tilde{\Lambda}_1(\tau), \dots, \tilde{\Lambda}_p(\tau) \right]^\top.$$

The kernel-weighted residuals $\Delta U_j K_h^{1/2}(t_j - \tau)$ in the local approximation (2.12) are then approximated by

$$\tilde{U}_j(\tau) = \left[\tilde{U}_{1,j}(\tau), \dots, \tilde{U}_{p,j}(\tau) \right]^\top = \Delta \tilde{X}_j K_h^{1/2}(t_j - \tau) - \tilde{\Lambda}(\tau) \Delta \tilde{F}_j(\tau),$$

which are subsequently used to estimate $\Sigma_U(\cdot)$. However, the conventional sample covariance matrix using $\tilde{U}_j(\tau)$:

$$\check{\Sigma}_U(\tau) = [\check{\sigma}_{U,i_1 i_2}(\tau)]_{p \times p} = \sum_{j=1}^N \tilde{U}_j(\tau) \tilde{U}_j(\tau)^\top, \quad (2.15)$$

usually performs poorly when the number of assets p is ultra large. To address this problem, we again apply the generalised shrinkage and estimate $\Sigma_U(\tau)$ by

$$\hat{\Sigma}_U(\tau) = [\hat{\sigma}_{U,i_1 i_2}(\tau)]_{p \times p} \quad \text{with} \quad \hat{\sigma}_{U,i_1 i_2}(\tau) = s_{\rho(\tau)}(\check{\sigma}_{U,i_1 i_2}(\tau)). \quad (2.16)$$

Finally, the estimate of $\Sigma_X(\tau)$ is obtained via

$$\hat{\Sigma}_X(\tau) = \tilde{\Lambda}(\tau) \tilde{\Lambda}(\tau)^\top + \hat{\Sigma}_U(\tau). \quad (2.17)$$

It is worth comparing our model assumption and methodology with those in [Chen, Mykland and Zhang \(2020\)](#) before concluding this section. Although our main model framework is similar to that in [Chen, Mykland and Zhang \(2020\)](#), we impose more general assumptions on the microstructure noises, allowing them to be nonlinear heteroskedastic and asymptotically vanishing. In particular, the noises can be endogenous but no explicit correlation structure (between noises and latent prices) is required. The estimation methodology in [Chen, Mykland and Zhang \(2020\)](#) is mainly built on the smoothed two-scale realised volatility introduced in [Chen, Mykland and Zhang \(2019\)](#), which combines the pre-averaging and two-scale realised volatility. This is further combined with local POET to estimate spot volatility matrices in the high dimension. In contrast, our proposed methodology is virtually simpler, using modified kernel weights in the first step of pre-averaging and kernel POET (or local PCA) in the second step.

3 Main theoretical results

In this section, we give some regularity conditions with remarks and then present the theoretical properties for the developed large spot volatility matrix estimates via the in-fill asymptotics.

3.1 Regularity conditions

Write

$$\begin{aligned}\mu_t^F &= (\mu_{1,t}^F, \dots, \mu_{k,t}^F)^\top, \quad \mu_t^U = (\mu_{1,t}^U, \dots, \mu_{p,t}^U)^\top, \\ \sigma_t^U &= (\sigma_{i_1 i_2, t}^U)_{p \times p}, \quad \Sigma_U(t) = [\sigma_{U, i_1 i_2}(t)]_{p \times p} = \sigma_t^U (\sigma_t^U)^\top.\end{aligned}$$

Assumption 1. (i) Let $\{\mu_{i,t}^F : t \geq 0\}$, $\{\mu_{i,t}^U : t \geq 0\}$, and $\{\sigma_{i_1 i_2, t}^U : t \geq 0\}$ be adapted locally bounded processes with continuous sample path.

(ii) Let $\{\sigma_{U, i_1 i_2}(t) : t \geq 0\}$, $1 \leq i_1, i_2 \leq p$, be adapted locally bounded and satisfy that

$$\min_{1 \leq i \leq p} \inf_{0 \leq t \leq T} \sigma_{U, ii}(t) > 0, \quad \min_{1 \leq i_1 \neq i_2 \leq p} \inf_{0 \leq t \leq T} [\sigma_{U, i_1 i_1}(t) + \sigma_{U, i_2 i_2}(t) + 2\sigma_{U, i_1 i_2}(t)] > 0,$$

and

$$\sup_{1 \leq i_1, i_2 \leq p} |\sigma_{U, i_1 i_2}(t + \epsilon) - \sigma_{U, i_1 i_2}(t)| \leq B_U(t, \epsilon) |\epsilon|^\delta + o(|\epsilon|^\delta), \quad \epsilon \rightarrow 0, \quad (3.1)$$

with probability one, where $0 < \delta < 1/2$, and $B_U(t, \epsilon)$ is a positive random function which is continuous with respect to t and slowly varying at $\epsilon = 0$.

(iii) Let $\{\Lambda_i(t) : t \geq 0\}$, $1 \leq i \leq p$, be adapted locally bounded processes satisfying that

$$\sup_{1 \leq i \leq p} \|\Lambda_i(t + \epsilon) - \Lambda_i(t)\| \leq B_\Lambda(t, \epsilon) |\epsilon|^\delta + o(|\epsilon|^\delta), \quad \epsilon \rightarrow 0, \quad (3.2)$$

with probability one, where $B_\Lambda(t, \epsilon)$ is defined similarly to $B_U(t, \epsilon)$ in (3.1), and

$$\sup_{0 \leq t \leq T} \left\| \frac{1}{p} \sum_{i=1}^p \Lambda_i(t) \Lambda_i(t)^\top - \Sigma_\Lambda(t) \right\| = o_p(1), \quad p \rightarrow \infty, \quad (3.3)$$

where $\Sigma_\Lambda(t)$ is positive definite with uniformly bounded eigenvalues.

Assumption 2. (i) Let $\{\varepsilon_{i,j}^* : j = 1, 2, \dots\}$ be a stationary and α -mixing random sequence satisfying that the mixing coefficient $\alpha_i(t) = O(\gamma_0^t)$ uniformly over i , $0 < \gamma_0 < 1$, $E(\varepsilon_{i,j}^*) = 0$, $\text{Var}(\varepsilon_{i,j}^*) = 1$ and

$$\max_{1 \leq i \leq p} E \left[\exp \{s_0 |\varepsilon_{i,j}^*|\} \right] \leq C_\varepsilon < \infty, \quad 0 < s_0 < \infty. \quad (3.4)$$

(ii) Let $0 \leq \beta_i < 1/2$ and the deterministic function $\chi_i(\cdot)$ satisfy that

$$\max_{1 \leq i \leq p} \sup_{0 \leq t \leq T} |\chi_i(t)| \leq C_\chi < \infty.$$

Assumption 3. (i) Let $t_j^i - t_{j-1}^i = c_j^i n_i^{-1}$, where

$$0 < \underline{c} \leq \min_{1 \leq i \leq p} \min_{1 \leq j \leq n_i} c_j^i \leq \max_{1 \leq i \leq p} \max_{1 \leq j \leq n_i} c_j^i \leq \bar{c} < \infty.$$

In addition, there exists a $\kappa_0 > 0$ such that $N = O(\underline{n}^{\kappa_0})$, where N is the number of pseudo-sampling time points in (2.8) and $\underline{n} = \min_{1 \leq i \leq p} n_i$.

(ii) The bandwidth b , the dimension p and the sample sizes n_i satisfy that $b \rightarrow 0$,

$$\min_{1 \leq i \leq p} \frac{n_i^{1-4\kappa_1} b}{\log(p \vee n_i)} \rightarrow \infty, \quad \sum_{i=1}^p n_i \exp\{-s_0 n_i^{\kappa_1}\} \rightarrow 0, \quad (3.5)$$

where $0 < \kappa_1 < 1/4$ and s_0 is defined in (3.4).

Assumption 4. (i) The kernels $L(\cdot)$ and $K(\cdot)$ are bounded and Lipschitz continuous probability density functions with a compact support $[-1, 1]$.

(ii) The bandwidth h , the dimension p and the pseudo-sample size N satisfy that

$$h^{2\delta} \log(p \vee N) \rightarrow 0, \quad \frac{Nh}{\log(p \vee N)} \rightarrow \infty, \quad \frac{ph}{\log^2(p \vee N) \varpi_p} \rightarrow \infty, \quad (3.6)$$

where ϖ_p is defined in (2.6). In addition,

$$N^{1/2} \bar{v}(p, b, \mathbf{n}) \rightarrow 0, \quad \bar{v}(p, b, \mathbf{n}) = \max_{1 \leq i \leq p} v(p, b, n_i), \quad (3.7)$$

where $\mathbf{n} = \{n_i\}_{i=1}^p$,

$$v(p, b, n_i) = \sqrt{\log(p \vee n_i)} \left[(n_i^{2\beta_i+1} b)^{-1/2} + (n_i b)^{-1} + b^{1/2} \right].$$

(iii) Let the time-varying tuning parameter $\rho(\cdot)$ in the generalised shrinkage be chosen as

$$\rho(\tau) = M(\tau) [\zeta_1(p, b, \mathbf{n}, N) + \zeta_2(p, h, N)],$$

where $M(\cdot)$ is a positive function satisfying that

$$0 < \underline{C}_M \leq \inf_{0 \leq t \leq T} M(t) \leq \sup_{0 \leq t \leq T} M(t) \leq \bar{C}_M < \infty,$$

$\zeta_1(p, b, n, N) = N^{1/2} \bar{v}(p, b, n)$ with $\bar{v}(p, b, n)$ defined in (3.7), and

$$\zeta_2(p, h, N) = \left(\frac{\omega_p}{ph} \right)^{1/2} + \left(\frac{\log(p \vee N)}{Nh} \right)^{1/2} + h^\delta.$$

Remark 3.1. (i) Assumption 1 contains some mild conditions on the drift, volatility and factor loading processes (e.g., Kong, 2018). In particular, the local boundedness conditions can be strengthened to the uniform boundedness via the localisation technique (e.g., Jacod and Protter, 2012):

$$\max_{1 \leq i \leq k} \sup_{0 \leq t \leq T} |\mu_{i,t}^F| + \max_{1 \leq i \leq p} \sup_{0 \leq t \leq T} |\mu_{i,t}^U| \leq C_\mu < \infty, \quad (3.8)$$

$$\max_{1 \leq i_1, i_2 \leq p} \sup_{0 \leq t \leq T} [|\sigma_{i_1 i_2, t}^U| + |\sigma_{U, i_1 i_2}(t)|] \leq C_\sigma < \infty, \quad (3.9)$$

$$\max_{1 \leq i \leq p} \sup_{0 \leq t \leq T} \|\Lambda_i(t)\| \leq C_\Lambda < \infty, \quad (3.10)$$

with probability one. The smoothness conditions (3.1) and (3.2) are similar to those in Kristensen (2010), Zu and Boswijk (2014) and Bu *et al.* (2023), which determine the bias order of the kernel-based estimation. The convergence assumption (3.3) is similar to the condition (3.1) in Wang *et al.* (2021), indicating that all the latent high frequency factors are pervasive if the minimum eigenvalue of $\Sigma_\Lambda(t)$ is bounded away from zero (uniformly over t).

(ii) Assumption 2 shows that the microstructure noise vector is allowed to be serially correlated, nonlinear heteroskedastic and asymptotically vanishing. We do not impose any explicit correlation structure between the noises and latent prices. The moment condition in (3.4) is weaker than the typical sub-Gaussian condition commonly adopted in high-dimensional covariance matrix estimation (e.g., Bickel and Levina, 2008). The restriction of $0 \leq \beta_i < 1/2$ in Assumption 2(ii) is the same as that in Kalnina and Linton (2008), and the uniform boundedness condition on $\chi_i(\cdot)$ parallels those in (3.8)–(3.10).

(iii) Assumption 3(i) imposes some mild restrictions on the transaction time points which are allowed to be non-equidistant (for each asset). The liquidity level of the asynchronous high-frequency data may vary over assets. For synchronised data setting with $n_1 = \dots = n_p = n$, the conditions on b and p in Assumption 3(ii) can be simplified to

$$\frac{n^{1-4\kappa_1} b}{\log(p \vee n)} \rightarrow \infty \quad \text{and} \quad \frac{pn}{\exp\{s_0 n^{\kappa_1}\}} \rightarrow 0.$$

The first condition is comparable to the commonly-used bandwidth condition $nb/\log n$ if κ_1 tends to zero and p diverges at a polynomial rate of n , whereas the second one indicates that the number of assets can be ultra large, diverging at an exponential rate of n . Although the transaction times t_j^i

are assumed to be non-random, we conjecture that the methodology and theory may be applicable when the transaction times are stochastic (e.g., [Jacod, Li and Zheng, 2017, 2019](#); [Li and Linton, 2022, 2023](#)) with modified Assumption 3(i). For example, it is easy to verify the main theorems when the stochastic transaction times are independent of all the other random elements in the model and the conditions in Assumption 3(i) hold with probability one. A more challenging case of endogenous transaction times will be explored in our future studies.

(iv) Assumption 4(i) imposes some mild conditions for the kernel functions $K(\cdot)$ and $L(\cdot)$, which are satisfied for the commonly-used uniform and Epanechnikov kernels. Assumption 4(ii) imposes some conditions on h , p and the pseudo-sample size N in the kernel POET and local PCA. The first condition in (3.6) is to handle the kernel estimation bias order uniformly whereas the fourth condition ensures that the approximation error of the latent price by the kernel filter converges to zero. When p is of order higher than N and ϖ_p is bounded, the third condition in (3.6) is implied by the second one and thus can be removed. The restriction (3.7) ensures that the accumulation of pre-averaging approximation errors is “small” in the local PCA and kernel POET. Assumption 4(iii) is similar to Assumption 4(iii) in [Bu et al. \(2023\)](#). In addition, the developed methodology and theory continue to hold when the time-varying tuning parameter varies over entries of the spot volatility matrix. For instance, we may set $\rho_{i_1 i_2}(\tau) = \rho(\tau)[\widehat{\sigma}_{U, i_1 i_1}(\tau)\widehat{\sigma}_{U, i_2 i_2}(\tau)]^{1/2}$ and shrink the estimate of the (i_1, i_2) -entry to zero if the spot *correlation* is smaller than $\rho(\tau)$.

3.2 Asymptotic theorems

We next present the in-fill asymptotic properties of the proposed estimates, letting $t_j^i - t_{j-1}^i \rightarrow 0$ and thus $n_i \rightarrow \infty$ for each asset. Proposition 3.1 below gives the uniform approximation order of the latent price estimates by kernel-weighted pre-averaging.

Proposition 3.1. Suppose that Assumptions 1–3 and 4(i) are satisfied. Define

$$\mathcal{D}_i = \left\{ \max_{1 \leq j \leq N} \left| \widetilde{X}_{i, t_j} - X_{i, t_j} \right| > c_{\dagger} v(p, b, n_i) \right\},$$

where c_{\dagger} is a sufficiently large positive constant and $v(p, b, n_i)$ is defined in Assumption 4(ii). Then

$$P \left(\bigcup_{i=1}^p \mathcal{D}_i \right) \rightarrow 0, \text{ as } p, \underline{n} \rightarrow \infty, \quad (3.11)$$

where \underline{n} is defined in Assumption 3(i).

Remark 3.2. (i) The approximation rate in Proposition 3.1 is determined by the orders of p , n_i , b and the magnitude of β_i . When β_i approaches zero, $(n_i b)^{-1}$ is dominated by $(n_i^{2\beta_i+1} b)^{-1/2}$ and

thus $v(p, b, n_i) = [\log(p \vee n_i)]^{1/2} [(n_i^{2\beta_i+1}b)^{-1/2} + b^{1/2}]$. When β_i approaches $1/2$, $(n_i^{2\beta_i+1}b)^{-1/2}$ is of order smaller than $(n_i b)^{-1}$ and $v(p, b, n_i) = [\log(p \vee n_i)]^{1/2} [(n_i b)^{-1} + b^{1/2}]$. It follows from Proposition 3.1 that

$$\max_{1 \leq i \leq p} \max_{1 \leq j \leq N} |\tilde{X}_{i,t_j} - X_{i,t_j}| = O_P(\bar{v}(p, b, \mathbf{n})), \quad (3.12)$$

where $\bar{v}(p, b, \mathbf{n})$ is defined in (3.7).

(ii) We next discuss explicit uniform approximation rates for some special cases. When the liquidity level remains the same over assets and the homogeneity restriction is imposed on β_i , i.e., $n_1 = \dots = n_p = n$ and $\beta_1 = \dots = \beta_p = \beta$, by (3.12), we readily have that

$$\max_{1 \leq i \leq p} \max_{1 \leq j \leq N} |\tilde{X}_{i,t_j} - X_{i,t_j}| = O_P \left([\log(p \vee n)]^{1/2} [(n^{2\beta+1}b)^{-1/2} + (nb)^{-1} + b^{1/2}] \right).$$

This approximation rate may be faster than that obtained in Lemma B.1 of Bu *et al.* (2023) as β may be positive. When the noise is not shrinking, i.e., $\beta \equiv 0$, we obtain

$$\max_{1 \leq i \leq p} \max_{1 \leq j \leq N} |\tilde{X}_{i,t_j} - X_{i,t_j}| = O_P \left([\log(p \vee n)]^{1/2} [b^{1/2} + (nb)^{-1/2}] \right),$$

which is the same as Lemma B.1 in Bu *et al.* (2023) and comparable to the rate derived by Kanaya and Kristensen (2016) for univariate high-frequency data. Furthermore, setting $b = n^{-1/2}$ and assuming that p diverges at a polynomial rate of n , we obtain

$$\max_{1 \leq i \leq p} \max_{1 \leq j \leq N} |\tilde{X}_{i,t_j} - X_{i,t_j}| = O_P \left((\log n)^{1/2} n^{-1/4} \right).$$

We next derive the uniform convergence property of the estimated idiosyncratic spot volatility matrix $\hat{\Sigma}_U(\cdot)$ in both the max and spectral norms. Since $\tilde{\Sigma}_U(\cdot)$ is equivalent to $\hat{\Sigma}_U(\cdot)$, the following theorem continues to hold for $\tilde{\Sigma}_U(\cdot)$.

Theorem 3.1. *Suppose that Assumptions 1–4 are satisfied. Then we have*

$$\sup_{h \leq \tau \leq T-h} \left\| \hat{\Sigma}_U(\tau) - \Sigma_U(\tau) \right\|_{\max} = O_P(\zeta(p, b, h, \mathbf{n}, N)), \quad (3.13)$$

and

$$\sup_{h \leq \tau \leq T-h} \left\| \hat{\Sigma}_U(\tau) - \Sigma_U(\tau) \right\|_s = O_P \left(\omega_p [\zeta(p, b, h, \mathbf{n}, N)]^{1-q} \right), \quad (3.14)$$

where

$$\zeta(p, b, h, \mathbf{n}, N) = \zeta_1(p, b, \mathbf{n}, N) + \zeta_2(p, h, N)$$

with $\zeta_1(p, b, \mathbf{n}, N)$ and $\zeta_2(p, h, N)$ defined in Assumption 4(iii).

Remark 3.3. (i) The order $\zeta_1(p, b, \mathbf{n}, N)$ in the uniform convergence rates is due to the pre-averaging approximation error of the latent prices (e.g., Proposition 3.1 and Remark 3.2), whereas $\zeta_2(p, h, N)$ is the estimation error of the infeasible local PCA directly with latent prices. With an extra term $[\bar{\omega}_p/(ph)]^{1/2}$ in $\zeta_2(p, h, N)$, our uniform convergence rates are a bit slower than that in Theorem 2 of Bu *et al.* (2023). If, in addition, assuming $\bar{\omega}_p = o([p \log(p \vee N)/N]^{1/2})$ and $p \geq N$, we may simplify $\zeta_2(p, h, N)$ to

$$\zeta_2^*(p, h, N) = \left(\frac{\log(p \vee N)}{Nh} \right)^{1/2} + h^\delta, \quad (3.15)$$

where the two rates are due to the kernel estimation variance and bias, respectively. In particular, treating Nh as the “effective pseudo sample size” in kernel-weighted estimation, the first term on the right side of (3.15) is an optimal minimax rate for large volatility matrix estimation (e.g., Cai and Zhou, 2012).

(ii) We next derive an explicit uniform convergence rate for $\hat{\Sigma}_U(\cdot)$. For simplicity, we replace $\zeta_2(p, h, N)$ by $\zeta_2^*(p, h, N)$ defined in (3.15) in the following discussion, and assume that $q = 0$, $\bar{\omega}_p$ is bounded, $n_1 = \dots = n_p = n$ and $\beta_1 = \dots = \beta_p = \beta$. We next consider two scenarios: (a) $n^{1-2\beta}b \rightarrow \infty$, and (b) $n^{1-2\beta}b \rightarrow 0$.

- Scenario (a) often occurs when β is close to zero. In this case, $(nb)^{-1}$ is dominated by $(n^{2\beta+1}b)^{-1/2}$ and thus

$$\zeta_1(p, b, \mathbf{n}, N) = [N \log(p \vee n)]^{1/2} [(n^{2\beta+1}b)^{-1/2} + b^{1/2}].$$

Setting $b = n^{-(2\beta+1)/2}$ and $h = N^{-1/(2\delta+1)}$ with $N = n^{(2\beta+1)(2\delta+1)/[2(4\delta+1)]}$, the rate $\zeta(p, b, h, \mathbf{n}, N)$ in (3.13) and (3.14) becomes $n^{-(2\beta+1)\delta/[2(4\delta+1)]} [\log(p \vee n)]^{1/2}$. Furthermore, when $\beta = 0$ and δ approaches $1/2$, this rate would be close to $n^{-1/12}$ (ignoring the logarithmic rate), comparable to those derived by Zu and Boswijk (2014) and Kanaya and Kristensen (2016) in the univariate high-frequency data setting. In fact, this uniform convergence rate is also comparable to that obtained by Chen, Mykland and Zhang (2020). When the microstructure noise is shrinking, i.e., $\beta > 0$, our uniform convergence rates would be faster.

- Scenario (b) often occurs when β is close to $1/2$. In this case, $(n^{2\beta+1}b)^{-1/2}$ is dominated by $(nb)^{-1}$ and thus

$$\zeta_1(p, b, \mathbf{n}, N) = [N \log(p \vee n)]^{1/2} [(nb)^{-1} + b^{1/2}].$$

Setting $b = n^{-2/3}$ and $h = N^{-1/(2\delta+1)}$ with $N = n^{2(2\delta+1)/[3(4\delta+1)]}$, we may obtain that $\zeta(p, b, h, \mathbf{n}, N) = n^{-2\delta/[3(4\delta+1)]} [\log(p \vee n)]^{1/2}$ in (3.13) and (3.14) which does not rely on β . In particular, when δ approaches $1/2$, this rate would be close to $n^{-1/9}$ (ignoring the logarithmic rate).

We next explore the uniform convergence property of $\widehat{\Sigma}_X(\cdot)$. Due to the time-varying factor model structure (1.2) with the condition (3.3), the largest k eigenvalues are spiked, diverging at a rate of p . Consequently, the spot volatility matrix $\Sigma_X(\cdot)$ cannot be consistently estimated in the absolute term. Motivated by Fan, Liao and Mincheva (2013), we measure the matrix estimate $\widehat{\Sigma}_X(\tau)$ in the following (time-varying) relative error:

$$\left\| \widehat{\Sigma}_X(\tau) - \Sigma_X(\tau) \right\|_{\Sigma_X(\tau)} = \frac{1}{\sqrt{p}} \left\| \Sigma_X^{-1/2}(\tau) \widehat{\Sigma}_X(\tau) \Sigma_X^{-1/2}(\tau) - I_p \right\|_F.$$

Theorem 3.2. *Suppose that Assumptions 1–4 are satisfied. Then we have*

$$\sup_{h \leq \tau \leq T-h} \left\| \widehat{\Sigma}_X(\tau) - \Sigma_X(\tau) \right\|_{\max} = O_P(\zeta(p, b, h, \mathbf{n}, N)), \quad (3.16)$$

and

$$\sup_{h \leq \tau \leq T-h} \left\| \widehat{\Sigma}_X(\tau) - \Sigma_X(\tau) \right\|_{\Sigma_X(\tau)} = O_P\left(p^{1/2} [\zeta(p, b, h, \mathbf{n}, N)]^2 + \omega_p [\zeta(p, b, h, \mathbf{n}, N)]^{1-q}\right), \quad (3.17)$$

where $\zeta(p, b, h, \mathbf{n}, N)$ is defined in Theorem 3.1.

Remark 3.4. (i) The uniform convergence rate in the elementwise max norm is the same as that in (3.13). To guarantee uniform consistency in the relative error of matrix estimation, we need to assume that $p^{1/2}[\zeta(p, b, h, \mathbf{n}, N)]^2 = o(1)$ and $\omega_p[\zeta(p, b, h, \mathbf{n}, N)]^{1-q} = o(1)$, which restrict the divergence rate of the asset number p , see also the discussions in Fan, Liao and Mincheva (2013) and Wang *et al.* (2021).

(ii) The spot precision matrix, the inverse of the spot volatility matrix, plays an important role in optimal portfolio selection. It is natural to take the inverse of $\widehat{\Sigma}_X(\cdot)$ as the estimate of $\Sigma_X(\cdot)$. By (2.17) and the Sherman-Morrison-Woodbury formula, we may write

$$\widehat{\Sigma}_X^{-1}(\tau) = \widehat{\Sigma}_U^{-1}(\tau) - \widehat{\Sigma}_U^{-1}(\tau) \widetilde{\Lambda}(\tau) \left[I_k + \widetilde{\Lambda}(\tau)^\top \widehat{\Sigma}_U^{-1}(\tau) \widetilde{\Lambda}(\tau) \right]^{-1} \widetilde{\Lambda}(\tau)^\top \widehat{\Sigma}_U^{-1}(\tau).$$

Following the standard arguments (e.g., Fan, Liao and Mincheva, 2013; Chen, Mykland and Zhang, 2020; Wang *et al.*, 2021) and using Theorem 3.1 and some technical lemmas available in Appendix B of Li, Linton and Zhang (2024), we may show that

$$\sup_{h \leq \tau \leq T-h} \left\| \widehat{\Sigma}_X^{-1}(\tau) - \Sigma_X^{-1}(\tau) \right\|_s = O_P\left(\omega_p [\zeta(p, b, h, \mathbf{n}, N)]^{1-q}\right).$$

(iii) Chen, Mykland and Zhang (2020) derive the point-wise convergence rates for $\Sigma_X(\tau)$ (in the elementwise max form) and $\Sigma_U(\tau)$ (in the spectral norm). Theorems 3.1 and 3.2 strengthen

their results to the uniform convergence ones (via different estimation method and technique in proofs). Theorem 3.2 also establishes the uniform convergence property for $\widehat{\Sigma}_X(\cdot)$ in the relative error measurement.

4 Monte-Carlo simulation studies

4.1 Data generating process

We generate the latent price process X_t from a drift-free time-varying factor model:

$$dX_t = \Lambda(t) dW_t^F + \sigma_t^U dW_t^U, \quad (4.1)$$

where $\Lambda(t)$ is a $p \times k$ time-varying factor loading process, σ_t^U is a $p \times p$ (diagonal) idiosyncratic volatility process, W_t^F is a k -dimensional standard Brownian motion and W_t^U is a p -dimensional Brownian motion with covariance matrix Σ_p . The number of latent factors is $k = 3$. The time-varying factor loading matrix $\Lambda(t) = [\Lambda_{i,l}(t)]_{p \times k}$ is generated from

$$\Lambda_{i,l}^2(t) = b_{i,l} [a_{i,l} - \Lambda_{i,l}^2(t)] dt + \sigma_{i,l}^0 \Lambda_{i,l}(t) dW_{i,t}^F, \quad i = 1, \dots, p, \quad l = 1, 2, 3,$$

where $a_{i,1} = 0.01 + i/p$, $a_{i,2} = 0.0115 + i/p$, $a_{i,3} = 0.0105 + i/p$, $b_{i,1} = 0.006 + i/(100p)$, $b_{i,2} = 0.007 + i/(100p)$, $b_{i,3} = 0.008 + i/(100p)$, $\sigma_{i,1}^0 = 0.3 + i/(5p)$, $\sigma_{i,2}^0 = \sigma_{i,3}^0 = 0.4 + i/(5p)$, and $W_{i,t}^F$ is the i -th element of W_t^F . Define $\sigma_t^U = \text{diag}(\sigma_{1,t}^U, \dots, \sigma_{p,t}^U)$ with

$$(\sigma_{i,t}^U)^2 = [0.00053 + i/(100p)] [0.0017 + i/p - (\sigma_{i,t}^U)^2] dt + [0.0013 + i/(10p)] \sigma_{i,t}^U dW_{i,t}^U,$$

where $W_{i,t}^U$ is the i -th element of W_t^U . Choose $\Sigma_p = (\rho_{ij})_{p \times p}$ as a correlation matrix satisfying the banded structure (e.g., [Gvozdev and Artemova, 2017](#)):

$$\rho_{ij} = \begin{cases} \rho^{|i-j|} \cdot I(|i-j| \leq 3), & i \neq j, \\ 1, & i = j, \end{cases}$$

where $I(\cdot)$ is an indicator function and $\rho \sim U(0, 0.5)$. Consequently, the generated spot volatility structure has the following low-rank plus sparse decomposition:

$$\Sigma_X(\tau) = \Lambda(\tau) \Lambda(\tau)^\top + \sigma_\tau^U \Sigma_p \sigma_\tau^U = \Sigma_C(\tau) + \Sigma_U(\tau), \quad 0 < \tau < T. \quad (4.2)$$

The number of assets is set to be $p = 100, 300, 500$ and the simulation is repeated for 100 times. The sampling frequency Δ is set to be $1/(6.5 \times 60 \times 6)$, which is equivalent to sampling in every 10

seconds, setting T as one trading day and assuming there are 6.5 trading hours for each trading day.

In practice, different asset prices are often non-synchronized and contaminated by the micro-structure noise. We generate the contaminated data via model (2.1). Similar to Fan and Kim (2019), we generate $\varepsilon_{i,t}$ independently (over i and t) from $\sigma_\varepsilon \cdot N(0, \sigma_{ii}(t))$, where $\sigma_{ii}(t)$ is the i -th diagonal element of the true spot volatility matrix $\Sigma_X(\cdot)$ at time point t and σ_ε is the noise-to-signal ratio. The noise is thus correlated with the latent prices. We consider $\sigma_\varepsilon = 0.05, 0.1$ and 0.2 . To simulate the asynchronous data, we use p independent Poisson processes to generate the true data collection time points t_j^i (e.g., Barndorff-Nielsen *et al.*, 2011). Specifically, for the i -th asset, we control $\{t_j^i : j = 1, \dots, n_i\}$ by a Poisson process with mean $\lambda^i \sim U(1, 3)$, indicating that asset prices are randomly collected every 10 to 30 seconds and we expect to have $2340/\lambda^i$ observations on average for the i -th asset.

4.2 Spot volatility matrix estimates

Throughout the simulation studies, we only use the kernel POET estimation method since it is equivalent to the local PCA. To assess the impacts of micro-structure noise and asynchronicity, we consider the following two spot volatility matrix estimators.

- Contaminated but synchronised spot volatility estimate $\bar{\Sigma}_X^s(\tau)$. We consider the synchronised data collected at every 10 seconds and then apply the developed kernel POET to the contaminated prices.
- Contaminated and asynchronised spot volatility estimate $\bar{\Sigma}_X^a(\tau)$. We consider the asynchronous asset prices that are randomly collected every 10 to 30 seconds and then apply the kernel POET. It is expected that the resulting finite-sample performance would be worse than the synchronised spot volatility matrix estimate $\bar{\Sigma}_X^s(\tau)$.

We employ the following four shrinkage techniques in the spot idiosyncratic volatility matrix estimation: Smoothly Clipped Absolute Deviation (SCAD), adaptive-lasso (A-lasso), soft thresholding (Soft) and hard thresholding (Hard). In addition, to demonstrate effectiveness of the generalised shrinkage, we also consider the naive estimator as a benchmark that does not apply shrinkage to the spot idiosyncratic volatility matrix estimation.

For each τ , we use the eigenvalue-ratio criterion (e.g., Anh and Horenstein, 2013) to determine the number of latent factors. Let $\bar{\Sigma}_X^{(r)}(\cdot)$ and $\bar{\Sigma}_U^{(r)}(\cdot)$ be generic notation for estimates of $\Sigma_X^{(r)}(\cdot)$ and $\Sigma_U^{(r)}(\cdot)$, respectively, for the r -th replication. To measure the distance between the true spot

volatility matrices and the estimated ones, we compute the following two measurements: the mean spectral norm deviation (MSN_X) and the mean relative norm deviation (MRN_X) defined by

$$\begin{aligned}\text{MSN}_X &= \frac{1}{100} \sum_{r=1}^{100} \left(\frac{1}{10} \sum_{j=1}^{10} \left\| \bar{\Sigma}_X^{(r)}(\tau_j) - \Sigma_X^{(r)}(\tau_j) \right\|_s \right), \\ \text{MRN}_X &= \frac{1}{100} \sum_{r=1}^{100} \left(\frac{1}{10} \sum_{j=1}^{10} \left\| \bar{\Sigma}_X^{(r)}(\tau_j) - \Sigma_X^{(r)}(\tau_j) \right\|_{\Sigma_X^{(r)}(\tau_j)} \right),\end{aligned}$$

where $\left\| \bar{\Sigma}_X^{(r)}(\tau) - \Sigma_X^{(r)}(\tau) \right\|_{\Sigma_X^{(r)}(\tau)}$ is defined as in Theorem 3.2 for the r -th replication, and $\tau_j, j = 1, 2, \dots, 10$, are equidistant time points. To compare the performance of various shrinkage approaches in estimating idiosyncratic spot volatility matrices, we compute the following mean spectral norm for the idiosyncratic spot volatility matrices:

$$\text{MSN}_u = \frac{1}{100} \sum_{r=1}^{100} \left(\frac{1}{10} \sum_{j=1}^{10} \left\| \bar{\Sigma}_u^{(r)}(\tau_j) - \Sigma_u^{(r)}(\tau_j) \right\|_s \right).$$

4.3 Choice of the tuning parameters

It is well known that the nonparametric kernel-based estimation is sensitive to the bandwidth selection. In the developed estimation procedure, we need to carefully select two bandwidths: b and h , which are involved in the kernel-weighted pre-averaging (2.7) and realised volatility matrix (2.8), respectively.

As recommended by Kanaya and Kristensen (2016), we apply the cross-validation to select the optimal bandwidth in the local pre-averaging for each asset, i.e., for the i -th asset, obtain

$$b_{\text{opt}}^i = \arg \min_{b>0} \text{CV}_i(b), \quad \text{CV}_i(b) = \sum_{j=1}^{n_i} \left(Y_{i,t_j^i} - \tilde{X}_{i,-t_j^i} \right)^2 \mathbf{1} \{ T_l^i \leq t_j^i \leq T_u^i \},$$

where the truncation mechanism is used to avoid the kernel estimation boundary effect, $T_l^i = 0.05 \times T_i$, $T_u^i = 0.95 \times T_i$, and $\tilde{X}_{i,-t_j^i}$ is the leave-one-out kernel filter defined as in (2.7) but removing the observation at t_j^i .

In the low-dimensional data setting, we may select the optimal bandwidth entry by entry in the realised volatility matrix estimation. For example, as in Kristensen (2010) and Kanaya and

Kristensen (2016), for $1 \leq i_1, i_2 \leq p$, we obtain

$$h_{\text{opt}}^{i_1 i_2} = \arg \min_{h>0} \text{CV}_{i_1 i_2}(h), \quad \text{CV}_{i_1 i_2}(h) = \sum_{\tau_j} \left[\left(\Delta \tilde{X}_{\tau_j} \Delta \tilde{X}'_{\tau_j} / \Delta \right)_{i_1 i_2} - \tilde{\sigma}_{X, i_1 i_2, -\tau_j} \right]^2,$$

where $\tilde{\sigma}_{X, i_1 i_2, -\tau_j}$ is the (i_1, i_2) -entry of leave-one-out kernel-weighted realised co-volatility estimate. However, this bandwidth selection criterion is rather time consuming when the dimension p is large. Hence, we adopt the following criterion:

$$h_{\text{opt}} = \arg \min_{h>0} \text{CV}(h), \quad \text{CV}(h) = \sum_{i=1}^p \sum_{\tau_j} \left[\left(\Delta \tilde{X}_{\tau_j} \Delta \tilde{X}'_{\tau_j} / \Delta \right)_{ii} - \tilde{\sigma}_{X, ii, -\tau_j} \right]^2,$$

where we only evaluate the quadratic loss for the diagonal elements. To further speed up the computation, as recommended by Kanaya and Kristensen (2016), we may repeat the bandwidth selection processes over a small number of replications (say, 5) and then fix the optimal bandwidth as the average of the selected bandwidth values.

When applying the generalised shrinkage in the kernel POET, we need to choose an appropriate tuning parameter to control the shrinkage level. As recommended by Fan, Liao and Mincheva (2013) and Wang *et al.* (2021) and discussed in Remark 3.1(iv), we set

$$\rho_{ij}(\tau) = c_\rho [\tilde{\sigma}_{U, ii}(\tau) \tilde{\sigma}_{U, jj}(\tau)]^{1/2}, \quad i, j = 1, \dots, p$$

where c_ρ is the minimum positive number guaranteeing positive definiteness of the estimated spot idiosyncratic volatility matrix. Specifically, c_ρ is chosen such that

$$c_\rho = \inf \left\{ c > 0 : \lambda_{\min} \left\{ \left(\bar{\Sigma}_U^c(\tau) \right) \right\} > 0, \quad \bar{\Sigma}_U^c(\tau) = [\bar{\sigma}_{U, ij}^c(\tau)]_{p \times p} \right\},$$

where $\bar{\sigma}_{U, ij}^c(\tau)$ is defined as in (2.10) using $\rho_{ij}(\tau) = c[\tilde{\sigma}_{U, ii}(\tau) \tilde{\sigma}_{U, jj}(\tau)]^{1/2}$.

4.4 Simulation results

Tables 1 and 2 report the MSN_U values of the spot idiosyncratic volatility matrix estimation for the noise-contaminated synchronised and asynchronised data, respectively. In general, the use of shrinkage results in more accurate estimation than the naive one without shrinkage. The improvement by using the shrinkage becomes more significant as the dimension p increases. The SCAD and adaptive-lasso perform somewhat better than the other two shrinkage methods when the high-frequency data are synchronised (see Table 1), and the adaptive-lasso outperforms the other shrinkage methods when the data are asynchronised (see Table 2). It is unsurprising that the

MSN_U values increase as the dimension or the noise-to-signal ratio σ_ϵ increases.

Tables 3–6 present the estimation results for Σ_X . Tables 3 and 4 report the MSN_X measurements whereas Tables 5 and 6 report the MRN_X measurements. As in Tables 1 and 2, the spot volatility matrix estimation with the generalised shrinkage outperforms the naive estimation without shrinkage. The difference between the shrinkage estimation and the naive one is more significant in terms of MRN_X . Both MSN_X and MRN_X increase as the dimension p grows. In particular, this divergence pattern is more significant for MSN_X , which is not uncommon as the true spot volatility matrix is spiked with the largest k eigenvalues diverging at the same rate of p . Hence, as recommended in [Fan, Liao and Mincheva \(2013\)](#), it is more sensible to use the MRN_X to access the factor-based spot volatility matrix estimation. Among the four shrinkage techniques, the SCAD and adaptive-lasso shrinkage slightly outperform the soft and hard thresholding methods, and the hard thresholding often has the poorest performance (although it is still superior to the naive estimator). Due to the data asynchronisation, the MSN_X and MRN_X values in Tables 4 and 6 are larger than those provided in Tables 3 and 5. The patterns of the estimation performance and comparison are similar over different noise-to-signal ratios. In addition, both the MSN_X and MRN_X measurements increase as σ_ϵ increases from 0.05 to 0.2, which is expected as “larger” noise results in “larger” approximation errors of the first-step pre-averaging.

Table 1: MSN_U measurements of Σ_U for synchronised data

p	σ_ϵ	Naive	SCAD	A-Lasso	Soft	Hard
$p = 100$	0.05	0.0270	0.0248	0.0267	0.0260	0.0293
	0.1	0.0288	0.0266	0.0267	0.0280	0.0293
	0.2	0.0346	0.0300	0.0298	0.0326	0.0310
$p = 300$	0.05	0.0432	0.0291	0.0296	0.0297	0.0357
	0.1	0.0479	0.0284	0.0285	0.0287	0.0371
	0.2	0.0578	0.0365	0.0365	0.0362	0.0441
$p = 500$	0.05	0.0752	0.0298	0.030	0.030	0.0473
	0.1	0.0781	0.0308	0.0316	0.0310	0.0506
	0.2	0.0875	0.0378	0.0377	0.0379	0.0587

Table 2: MSN_U measurements of Σ_U for asynchronised data

p	σ_ϵ	Naive	SCAD	A-Lasso	Soft	Hard
$p = 100$	0.05	0.0409	0.0358	0.0357	0.0354	0.0374
	0.1	0.0418	0.0366	0.0363	0.0361	0.0381
	0.2	0.0425	0.0359	0.0355	0.0353	0.0380
$p = 300$	0.05	0.0800	0.0455	0.0446	0.0454	0.0610
	0.1	0.0802	0.0461	0.0451	0.0459	0.0614
	0.2	0.0872	0.0461	0.0450	0.0460	0.0648
$p = 500$	0.05	0.1327	0.0599	0.0586	0.0600	0.0941
	0.1	0.1340	0.0605	0.0592	0.0605	0.0947
	0.2	0.1345	0.0599	0.0867	0.0600	0.0950

Table 3: MSN_X measurements of Σ_X for synchronised data

p	σ_ϵ	Naive	SCAD	A-Lasso	Soft	Hard
$p = 100$	0.05	1.7758	1.7728	1.7724	1.7750	1.7740
	0.1	1.8359	1.8323	1.8317	1.8356	1.8320
	0.2	2.1769	2.1723	2.1715	2.1756	2.1720
$p = 300$	0.05	5.2782	5.2734	5.2732	5.2738	5.2755
	0.1	5.4809	5.4721	5.4713	5.4731	5.4751
	0.2	6.5930	6.5833	6.5823	6.5837	6.5865
$p = 500$	0.05	8.645	8.6364	8.6365	8.6366	8.6388
	0.1	8.9720	8.9622	8.9618	8.9627	8.9660
	0.2	10.7411	10.7303	10.7294	10.7305	10.7343

Table 4: MSN_X measurements of Σ_X for asynchronised data

p	σ_ϵ	Naive	SCAD	A-Lasso	Soft	Hard
p = 100	0.05	2.3825	2.3810	2.3807	2.3808	2.3812
	0.1	2.3855	2.3841	2.3839	2.3840	2.3845
	0.2	2.3885	2.3869	2.3867	2.3870	2.3873
p = 300	0.05	7.1376	7.1357	7.1357	7.1357	7.1367
	0.1	7.1412	7.1396	7.1396	7.1397	7.1405
	0.2	7.1415	7.1399	7.1399	7.1400	7.1408
p = 500	0.05	11.6455	11.6437	11.6439	11.6440	11.6450
	0.1	11.6468	11.6453	11.6459	11.6454	11.6463
	0.2	11.6470	11.6454	11.6456	11.6454	11.6464

Table 5: MRN_X measurements of Σ_X for synchronised data

p	σ_ϵ	Naive	SCAD	A-Lasso	Soft	Hard
p = 100	0.05	1.6260	1.4179	1.4078	1.5433	1.4910
	0.1	2.2902	2.1172	2.1117	2.2680	2.2000
	0.2	2.8643	2.5876	2.7683	2.2904	2.6516
p = 300	0.05	2.9659	2.2503	2.2019	2.2904	2.5560
	0.1	3.4108	2.7957	2.7707	2.8200	3.0466
	0.2	4.0430	3.3056	3.0117	3.0812	3.4895
p = 500	0.05	3.9195	2.9387	2.8699	2.9416	3.3836
	0.1	4.5601	3.5998	3.5648	3.6178	4.0260
	0.2	5.3357	4.2404	4.2161	4.2471	4.7475

Table 6: MRN_X measurements of Σ_X for asynchronised data

p	σ_ϵ	Naive	SCAD	A-Lasso	Soft	Hard
p = 100	0.05	2.7097	2.4809	2.4691	2.4650	2.5816
	0.1	2.7484	2.5469	2.5359	2.5354	2.6380
	0.2	3.0464	2.8049	2.7930	2.7900	2.9100
p = 300	0.05	4.0469	4.4397	3.4174	3.4388	3.7649
	0.1	4.0880	4.4732	3.4504	3.4722	3.8022
	0.2	4.5535	3.8059	3.7795	3.8054	4.2053
p = 500	0.05	6.2918	5.1528	5.1268	5.1525	5.7603
	0.1	6.3458	5.2133	5.1874	5.2130	5.8156
	0.2	6.6000	5.4200	5.3920	5.4186	6.0456

5 An empirical application

We next apply the proposed approach to the one-min intraday log-price of S&P 500 index constituents. The log-prices are extracted from Bloomberg, ranging from 29 March to 30 June 2021. There are 66 trading days and 505 stocks in total. The 66 trading days are divided into 11 equal-length time intervals, with 6 trading days in each time interval. In the preliminary data analysis, we remove the illiquid stocks that were not traded for more than half of one-minute trading periods on each trading day, resulting in 353 stocks in total. We also exclude stock prices that are outside the trading hours of 9:30 am (EST) to 4 pm (EST). A recent paper by [Li, Chen and Linton \(2023\)](#) estimates the latent factor structure for the same data set, allowing the existence of microstructure noises. In this section, we aim to further explore the spot volatility structure and study its time-varying pattern. For each equal-length time interval, we first apply the kernel-weighted pre-averaging method in (2.7) to the (noisy) log-price and then construct the kernel-weighted spot volatility matrix estimates in (2.8). Due to a possible low-rank plus sparse structure, we further implement the kernel POET estimation as in (2.11). Specifically, we estimate 36 evenly separated spot volatility matrices in each time interval (i.e., 6 spot volatility matrix estimates for each trading day). As recommended in the simulation, we adopt the adaptive-lasso in the generalised shrinkage with the tuning parameter chosen according to the criteria discussed in Section 4.3.

The left panel of Figure 1 depicts the log-price of the POOL.OQ stock over the sampling period whereas the right panel depicts the fitted log-price via the kernel-weighted pre-averaging. We use the Gaussian kernel function in (2.7) and determine the optimal bandwidth via the cross-validation discussed in Section 4.3. It follows from Figure 1 that the fitted log-prices are generally close to the

original ones which may be noise contaminated, capturing most of the dynamic patterns. Due to the kernel-weighted smoothing, the fitted prices are slightly smoother than the observed ones.

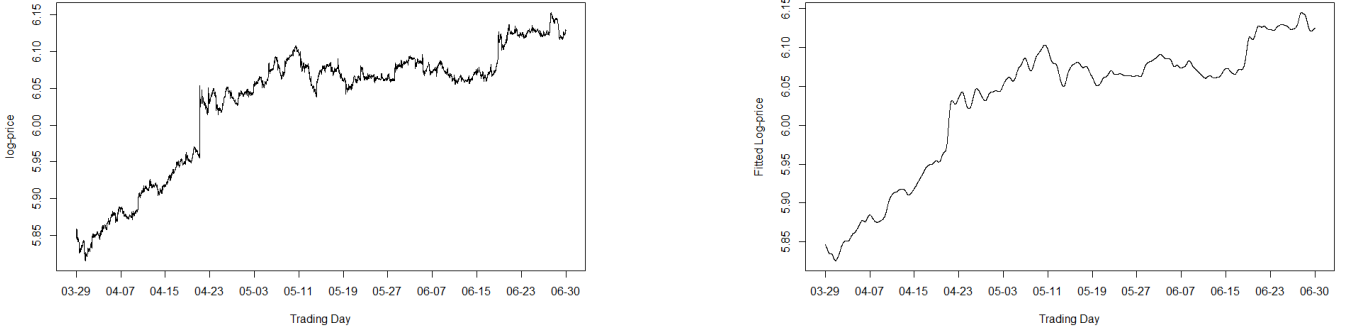


Figure 1: The left panel is the plot of the POOL.OQ stock (log) price and the right panel is the plot of the fitted log-price via pre-averaging.

With the kernel POET estimates in (2.11), we are able to collect the estimated spot volatilities (the diagonal entries of the estimated spot volatility matrix) for all the stocks and the estimated spot covariances (the off-diagonal entries of the estimated spot volatility matrix) between every pair of stocks across all the trading days. We further average the estimated volatilities and covariances within each trading day over the sampling period, and rank them (in decreasing order) according to variances of all the realised volatility and covariance over time. The estimated volatilities and covariances of the 20%, 40%, 60% and 80% quantile stocks (or stock pairs) across all the trading days are plotted in Figures 2 and 3, respectively. It follows from the plots that both the spot volatilities and covariances exhibit significant dynamic changes over time, demonstrating that it is imperative to recover the spot volatility structure over time for high-frequency financial data.

Figure 4 plots the heat maps for the estimated spot correlation matrices on two typical trading days: 19 May and 7 June. The heat maps in the upper panel are obtained for 7 June, which represents a typical period of stable volatility with nine estimated common factors. In contrast, those in the lower panel are for 19 May, which corresponds to the period during the crypto-currency market collapse (e.g., Pound, 2021) with only two estimated common factors. We note that the upper-left heat map (with nine estimated factors) is slightly denser than the lower-left one (with two estimated factors), which may be partly explained by the magnitude of the market disruption. During the period of the crypto-currency market collapse, its disruption is so large that it nearly dominates the entire stock market. Consequently, the two estimated factors can explain majority of the market volatility. In contrast, the nine estimated factors during the stable period may only explain a limited portion of the market volatility. Therefore, it is reasonable to expect that the spot idiosyncratic correlation matrix tends to be more sparse (after removing the latent factors) when

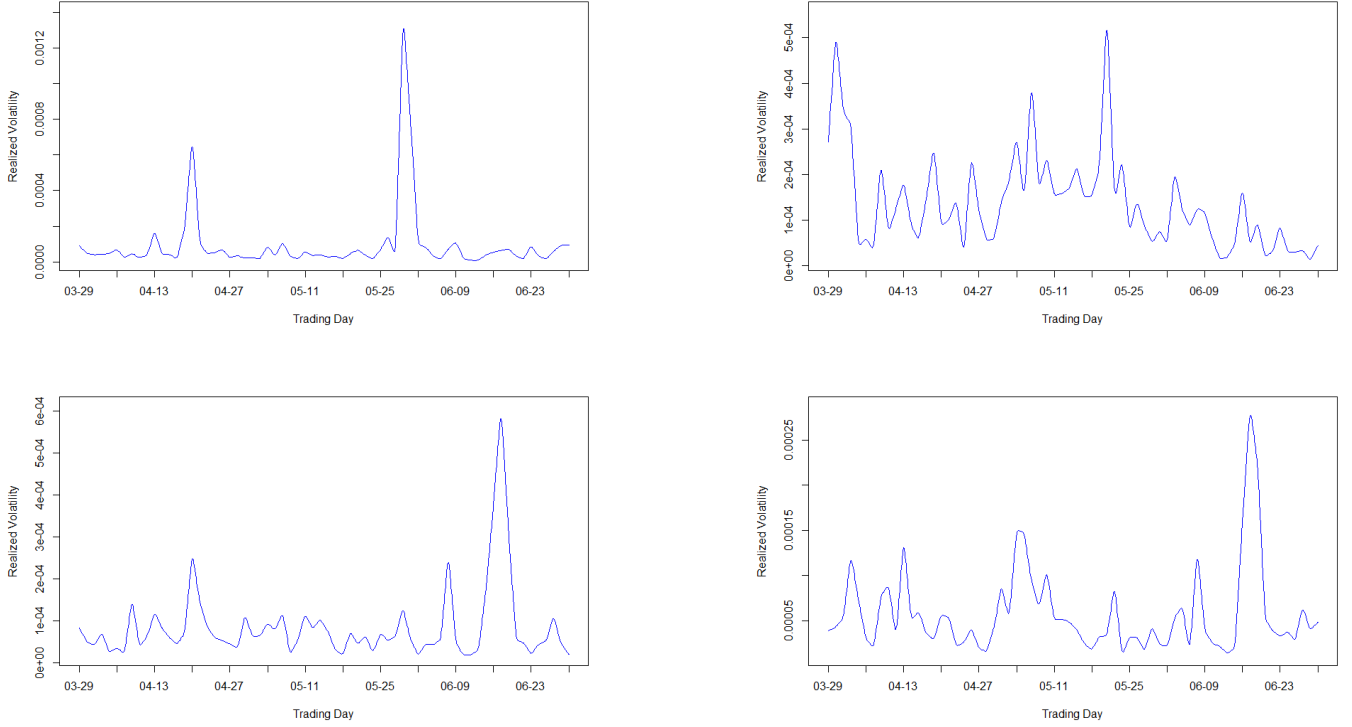


Figure 2: Plots of the estimated spot volatility of 20%-th, 40%-th, 60%-th and 80%-th quantile stocks. Upper-left panel: plot of the estimated spot volatility of ABT.N stock (20%-th quantile); upper-right panel: plot of the estimated spot volatility of SNPS.OQ stock (40%-th quantile); lower-left panel: plot of the estimated spot volatility of MET.N stock (60%-th quantile); lower-right panel: plot of the estimated spot volatility of EMR.N stock (80%-th quantile).

the market collapses. In fact, by applying the shrinkage, the sparse structure of both the heat maps in the right panel is apparent, in which majority of the off-diagonal entries are either zero or very close to zero. This supports the low-rank plus sparse assumption on the spot volatility structure.

We next further study the time-varying pattern of the factor number estimation and its connection to the market volatility. The left panel in Figure 5 plots the averages of the estimated factor numbers over the six pre-determined time intervals in each trading day, and the right panel depicts the realised volatility of the S&P 500 index intraday prices across trading days. It is well known that the S&P 500 index is a market value-weighted index and is thus regarded as an indicator of the entire stock market in US. A virtual comparison between the two plots in Figure 5 reveals that the averaged factor number tends to be low when the realised volatility of S&P 500 index is high, whereas the estimated factor number is relatively high when the market realised volatility is low. This pattern is not uncommon in the financial market as the extreme fluctuation in the financial market is often closely correlated with some unexpected financial events or economic disruption. Consequently, a small number of factors tend to dominate the market during the period of market

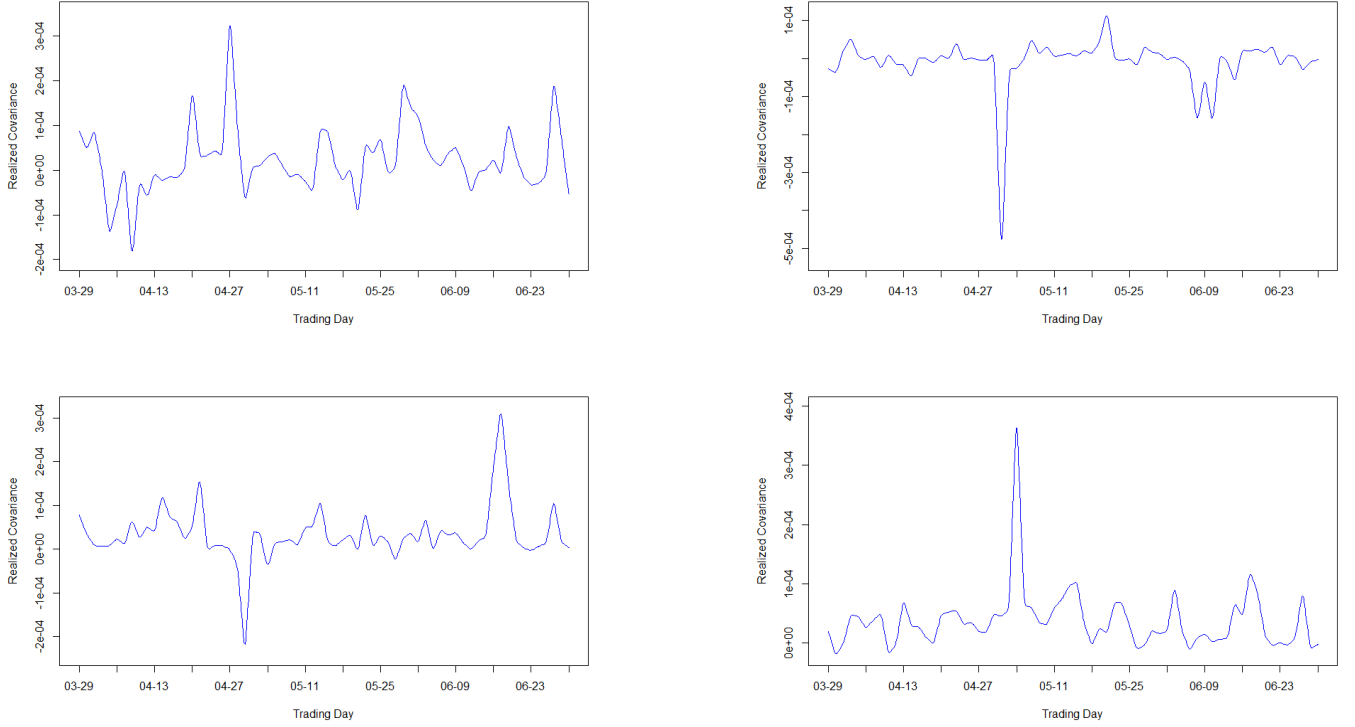


Figure 3: Plots of the estimated spot covariances of the 20%-th, 40%-th, 60%-th and 80%-th quantile stock pairs. Upper-left panel: plot of the estimated spot covariance between APA.OQ and MA.N stocks (20%-th quantile); upper-right panel: plot of the estimated spot covariance between VRTX.OQ and FTV.N stocks (40%-th quantile); lower-left panel: plot of the estimated spot covariance between BWA.N and CB.N stocks (60%-th quantile); lower-right panel: plot of the estimated spot covariance between CTVA.N and D.N stocks (80%-th quantile).

collapse. For example, in May 2021, the crypto-currency market collapsed for the first time, and this shock rapidly spread to the entire stock market. This adequately explains the peak of the realised volatility and the low estimated factor number in the midst of May which can be observed in Figure 5. In contrast, when the financial market is relatively stable, more factors tend to affect the market simultaneously, which is exactly what occurred at the end of May and the beginning of June in 2021.

6 Conclusion

In this paper we propose a new nonparametric methodology and theory for estimating the low-rank plus sparse spot volatility structure of the noise-contaminated and asynchronous high-frequency data with large dimension. The microstructure noises are allowed to be auto-correlated,

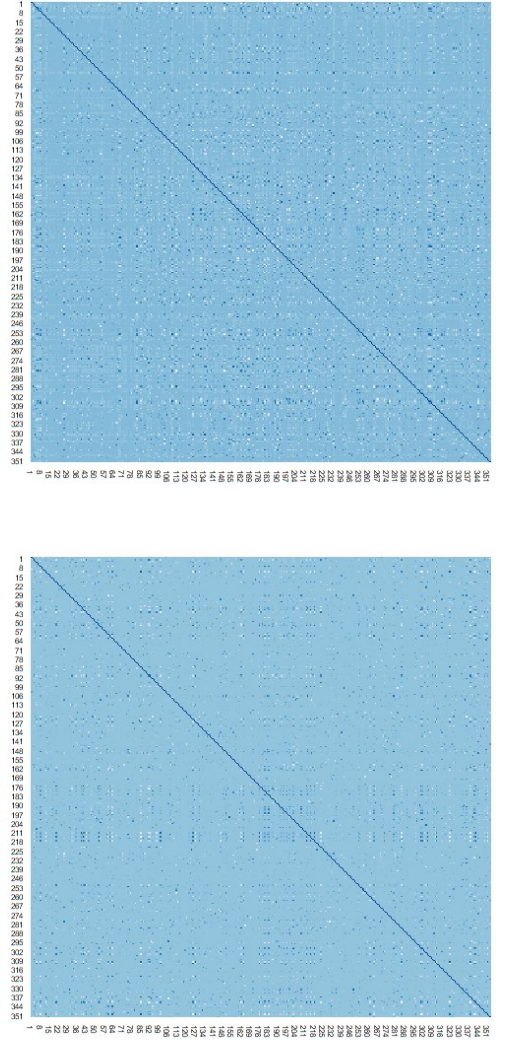
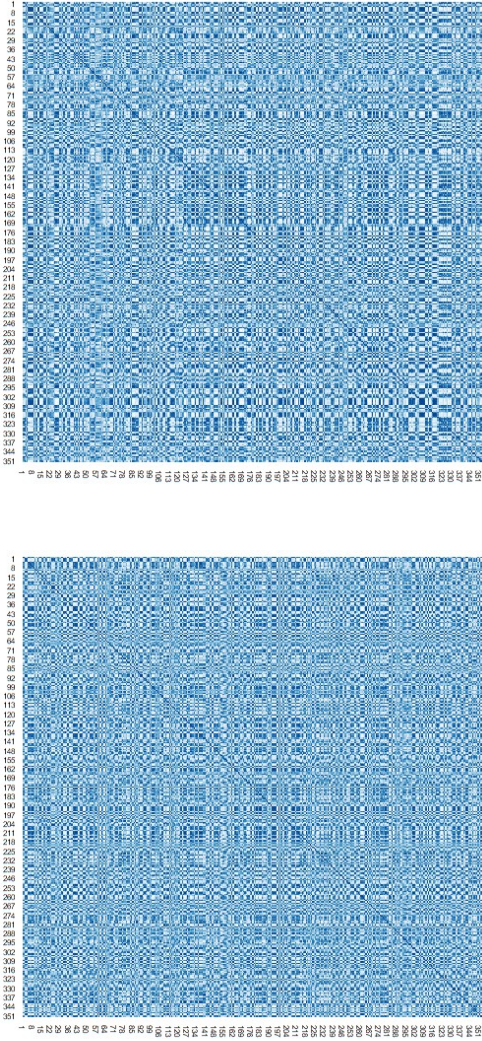


Figure 4: The upper panel is the heat maps of the estimated spot volatility matrices for the log prices (left) and idiosyncratic components (right) on 7 June, and the lower panel is the heat maps of the estimated spot volatility matrices for the log prices (left) and idiosyncratic components (right) on 19 May. The shrinkage technique is used to estimated the spot idiosyncratic volatility matrices.

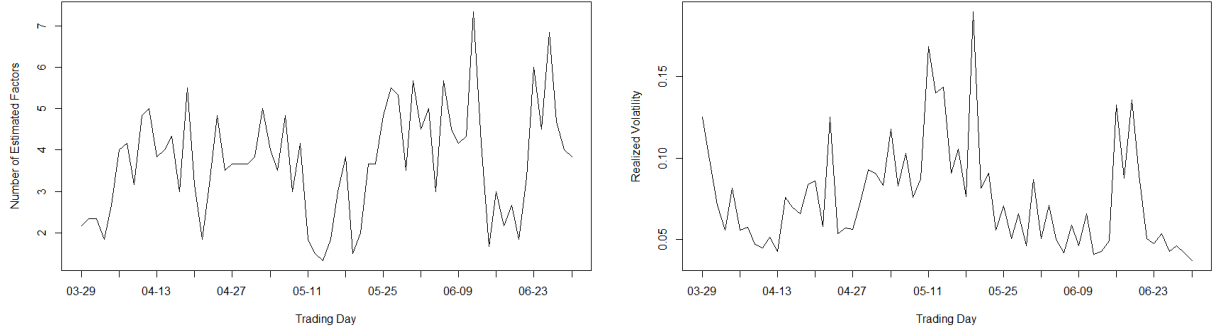


Figure 5: The left panel is the plot of the (time-varying) estimated number of factors (averaged over each trading day), and the right panel is the plot of the realised volatility based on 1-min intraday stock price of S&P 500 index over the sampling period.

nonlinear heteroskedastic, asymptotic vanishing and endogenous, and the latent prices satisfy the time-varying continuous-time factor model. Imposing the sparsity restriction on the spot idiosyncratic volatility matrix, we combine the kernel-weighted POET (or local PCA) and pre-averaging techniques to develop the main estimation method. Under some regularity conditions, we derive the uniform convergence property for the estimated spot volatility matrix in various matrix norms and obtain some explicit convergence rates for different scenarios. The Monte-Carlo simulation study shows that the developed estimation method performs well in finite samples. In particular, the empirical application to the S&P 500 index reveals time-varying patterns of the spot volatility matrix and latent factor number and confirms rationality of assuming the low-rank plus sparse structure.

Acknowledgement

The first author's research was partly supported by the Leverhulme Research Fellowship (RF-2023-396) and BA/Leverhulme Small Research Grant (SRG1920/100603).

Supplementary material

The supplement contains the proofs of the main theoretical results (in Appendix A) and some technical lemmas with proofs (in Appendix B).

References

- AÏT-SAHALIA, Y. AND JACOD, J. (2014). *High-Frequency Financial Econometrics*. Princeton University Press.
- AÏT-SAHALIA, Y. AND XIU, D. (2017). Using principal component analysis to estimate a high dimensional factor model with high-frequency data. *Journal of Econometrics* **201**, 384–399.
- ANDERSEN, T. G., BOLLERSLEV, T., DIEBOLD, F. X. AND LABYS, P. (2003). Modeling and forecasting realized volatility. *Econometrica* **71**, 579–625.
- AHN, S. AND HORENSTEIN, A. (2013). Eigenvalue ratio test for the number of factors. *Econometrica* **81**, 1203–1227.
- BAI, J. AND NG, S. (2002). Determining the number of factors in approximate factor models. *Econometrica* **90**, 191–221.
- BANDI, F. AND RENÒ, R. (2018). Nonparametric stochastic volatility. *Econometric Theory* **34**, 1207–1255.
- BARNDORFF-NIELSEN, O. E. AND SHEPHARD, N. (2002). Econometric analysis of realized volatility and its use in estimating stochastic volatility models. *Journal of the Royal Statistical Society Series B* **64**, 253–280.
- BARNDORFF-NIELSEN, O. E. AND SHEPHARD, N. (2004). Econometric analysis of realized covariation: High frequency based covariance, regression and correlation in financial economics. *Econometrica* **72**, 885–925.
- BARNDORFF-NIELSEN, O. E., HANSEN, P. R., LUNDE, A. AND SHEPHARD, N. (2011). Multivariate realised kernels: Consistent positive semi-definite estimators of the covariation of equity prices with noise and non-synchronous trading. *Journal of Econometrics* **162**, 149–169.
- BICKEL, P. AND LEVINA, E. (2008). Covariance regularization by thresholding. *The Annals of Statistics* **36**, 2577–2604.
- BOSQ, D. (1998). *Nonparametric Statistics for Stochastic Processes: Estimation and Prediction*. Springer.
- BU, R., LI, D., LINTON, O. AND WANG, H. (2023). Nonparametric estimation of large spot volatility matrices for high-frequency financial data. Working paper available at <https://arxiv.org/abs/2307.01348>.
- CAI, T. T., HU, J., LI, Y. AND ZHENG, X. (2020). High-dimensional minimum variance portfolio estimation based on high-frequency data. *Journal of Econometrics* **214**, 482–494.
- CAI, T. T. AND ZHOU, H. H. (2012). Optimal rates of convergence for sparse covariance matrix estimation. *The Annals of Statistics* **40**, 2389–2420.
- CHAMBERLAIN, G. AND ROTHSCILD, M. (1983). Arbitrage, factor structure and mean-variance analysis in large asset markets. *Econometrica* **51**, 1305–1324.

- CHEN, D., MYKLAND, P. AND ZHANG, L. (2019). The algebra of two scales estimation and the S-TSRV: High frequency estimation that is robust to sampling times. *Journal of Econometrics* **208**, 101–119.
- CHEN, D., MYKLAND, P. AND ZHANG, L. (2020). The five trolls under the bridge: Principal component analysis with asynchronous and noisy high frequency data. *Journal of the American Statistical Association* **115**, 1960–1977.
- CHEN, D., MYKLAND, P. AND ZHANG, L. (2023). Realized regression with asynchronous and noisy high frequency and high dimensional data. Forthcoming in *Journal of Econometrics*.
- CHEN, J., LI, D. AND LINTON, O. (2019). A new semiparametric estimation approach of large dynamic covariance matrices with multiple conditioning variables. *Journal of Econometrics* **212**, 155–176.
- CHEN, X., XU, M. AND WU, W. (2013). Covariance and precision matrix estimation for high-dimensional time series. *Annals of Statistics* **41**, 2994–3021.
- CHEN, Z. AND LENG, C. (2016). Dynamic covariance models. *Journal of the American Statistical Association* **111**, 1196–1207.
- CHRISTENSEN, K., KINNEBROCK, S. AND PODOLSKIJ, M. (2010). Pre-averaging estimators of the ex-post covariance matrix in noisy diffusion models with non-synchronous data. *Journal of Econometrics* **159**, 116–133.
- DA, R. AND XIU, D. (2021). When moving-average models meet high-frequency data: Uniform inference on volatility. *Econometrica* **89**, 2787–2825.
- DAI, C., LU, K. AND XIU, D. (2019). Knowing factors or factor loadings, or neither? Evaluating estimators for large covariance matrices with noisy and asynchronous data. *Journal of Econometrics* **208**, 43–79.
- DAVIS, C. AND KAHAN, W. M. (1970). The rotation of eigenvectors by a perturbation. III. *SIAM Journal on Numerical Analysis* **7**, 1–46.
- DEMIGUEL, V., GARLAPPI, L., NOGALES, F.J. AND UPPAL, R. (2009). A generalized approach to portfolio optimization: improving performance by constraining portfolio norms *Management Science* **55**, 798–812.
- DING, Y., LI, Y. AND ZHENG, X. (2021). High dimensional minimum variance portfolio estimation under statistical factor models *Journal of Econometrics* **222**, 502–515.
- EPPS, T. W. (1979). Comovements in stock prices in the very short run. *Journal of the American Statistical Association* **74**, 291–298.
- FAN, J., FAN, Y. AND LV, J. (2008). High dimensional covariance matrix estimation using a factor model. *Journal of Econometrics* **147**, 186–197.

- FAN, J., FURGER, A. AND XIU, D. (2016). Incorporating global industrial classification standard into portfolio allocation: A simple factor-based large covariance matrix estimator with high frequency data. *Journal of Business and Economic Statistics* **34**, 489–503.
- FAN, J., LI, Y. AND YU, K. (2012). Vast volatility matrix estimation using high-frequency data for portfolio selection. *Journal of the American Statistical Association* **107**, 412–428.
- FAN, J., LIAO, Y. AND MINCHEVA, M. (2013). Large covariance estimation by thresholding principal orthogonal complements (with discussion). *Journal of the Royal Statistical Society, Series B* **75**, 603–680.
- FAN, J. AND KIM, D. (2019). Structured volatility matrix estimation for nonsynchronized high-frequency financial data. *Journal of the Econometrics* **209**, 61–78.
- FAN, J. AND WANG, Y. (2008). Spot volatility estimation for high-frequency data. *Statistics and Its Interface* **1**, 279–288.
- GVOZDAREV, A. AND ARTEMOVA, R. (2017). Banded correlation matrix model for massive MIMO systems. *IEEE East-West Design and Test Symposium (EWDTS)*, 1–6.
- HANSEN, P. R. AND LUND, A. (2006). Realized variance and market microstructure noise (with comments and rejoinder). *Journal of Business and Economic Statistics* **24**, 127–218.
- JACOD, J., LI, Y., MYKLAND, P. A., PODOLSKIJ, M. AND VETTER, M. (2009). Microstructure noise in the continuous case: the pre-averaging approach. *Stochastic Processes and Their Applications* **119**, 2249–2276.
- JACOD, J., LI, Y. AND ZHENG, X. (2017). Statistical properties of microstructure noise. *Econometrica* **85**, 1133–1174.
- JACOD, J., LI, Y. AND ZHENG, X. (2019). Estimating the integrated volatility with tick observations. *Journal of Econometrics* **208**, 80–100.
- JACOD, J. AND PROTTER, P. (2012). *Discretization of Processes*. Springer.
- KALNINA, I. AND LINTON, O. (2008). Estimating quadratic variation consistently in the presence of endogenous and diurnal measurement error. *Journal of Econometrics* **147**, 47–59.
- KANAYA, S. AND KRISTENSEN, D. (2016). Estimation of stochastic volatility models by nonparametric filtering. *Econometric Theory* **32**, 861–916.
- KIM, D., WANG, Y. AND ZOU, J. (2016). Asymptotic theory for large volatility matrix estimation based on high-frequency financial data. *Stochastic Processes and Their Applications* **126**, 3527–3577.
- KONG, X. (2018). On the systematic and idiosyncratic volatility with large panel high-frequency data. *Annals of Statistics* **46**, 1077–1108.

- KONG, X. AND LIU, C. (2018). Testing against constant factor loading matrix with large panel high-frequency data. *Journal of Econometric* **204**, 301–319.
- KRISTENSEN, D. (2010). Nonparametric filtering of the realized spot volatility: a kernel-based approach. *Econometric Theory* **26**, 60–93.
- LEE, S. S. AND MYKLAND, P. A. (2007). Jumps in financial markets: a new nonparametric test and jump dynamics. *Review of Financial Studies* **21**, 2535–2563.
- LI, Y., CHEN, J. AND LINTON, O. (2023). Estimation of common factors for microstructure noise and efficient price in a high-frequency dual factor model. Forthcoming in *Journal of Econometrics*.
- LI, D., LINTON, O. AND ZHANG, H. (2024). Supplement to “Estimating Factor-Based Spot Volatility Matrices with Noisy and Asynchronous High-Frequency Data”.
- LI, Z. M. AND LINTON, O. (2022a). A ReMeDI for microstructure noise. *Econometrica* **90**, 367–389.
- LI, Z. M. AND LINTON, O. (2023). Robust estimation of integrated and spot volatility. Forthcoming in *Journal of Econometrics*.
- MOTTA, G., HAFNER, C. AND VON SACHS, R. (2011). Local stationary factor models: identification and nonparametric estimation. *Econometric Theory* **27**, 1279–1319.
- PELGER, M. (2019). Large-dimensional factor modeling based on high-frequency observations. *Journal of Econometrics* **208**, 23–42.
- POUND, J. (2021). The crypto collapse: Here’s what’s behind bitcoin’s sudden drop. *CNBC*, 19 May.
- SHEPHARD, N. (2005). *Stochastic Volatility: Selected Readings*. Oxford University Press.
- SU, L. AND WANG, X. (2017). On time-varying factor models: estimation and testing. *Journal of Econometrics* **198**, 84–101.
- SUN, Y. AND XU, W. (2022). A factor-based estimation of integrated covariance matrix with noisy high-frequency data. *Journal of Business and Economic Statistics* **40**, 770–784.
- WANG, H., PENG, B., LI, D. AND LENG, C. (2021). Nonparametric estimation of large covariance matrices with conditional sparsity. *Journal of Econometrics* **223**, 53–72.
- ZHANG, L. (2011). Estimating covariation: Epps effect, microstructure noise. *Journal of Econometrics* **160**, 33–37.
- ZHANG, L., MYKLAND, P. A. AND AÏT-SAHALIA, Y. (2005). A tale of two time scales: Determining integrated volatility with noisy high-frequency data. *Journal of the American Statistical Association* **100**, 1394–1411.
- ZU, Y. AND BOSWIJK, H. P. (2014). Estimating spot volatility with high-frequency financial data. *Journal of Econometrics* **181**, 117–135.

Supplementary Material to “Estimating Factor-Based Spot Volatility Matrices with Noisy and Asynchronous High-Frequency Data”

A Proofs of the main theoretical results

Unless explicitly stated differently, all the equations, propositions, remarks, theorems and lemmas mentioned in this appendix refer to those presented in the main text. In this appendix, we provide the detailed proofs of the main theoretical results stated in Section 3. As discussed in Remark 3.1, the local boundedness conditions on $\mu_{i,t}^F$, $\mu_{i,t}^U$, $\sigma_{i_1 i_2, t}^U$, $\sigma_{U, i_1 i_2}(t)$ and $\Lambda_i(t)$ in Assumption 1 can be strengthened to the uniform boundedness conditions over the entire time interval, i.e., (3.8)–(3.10) in main text hold. Throughout the proofs, we let C be a generic positive constant whose value may change from line to line.

A.1 Proof of Proposition 3.1

By model (2.1) and the definition of $\tilde{X}_{i,t}$ in (2.7), we obtain the following decomposition:

$$\tilde{X}_{i,t_i} - X_{i,t_i} = \Pi_{i,l}(1) + \Pi_{i,l}(2) + \Pi_{i,l}(3) + \Pi_{i,l}(4), \quad (\text{A.1})$$

where

$$\begin{aligned} \Pi_{i,l}(1) &= \sum_{j=1}^{n_i} (t_j^i - t_{j-1}^i) L_b(t_j^i - t_l) \varepsilon_{i,j}, \\ \Pi_{i,l}(2) &= \sum_{j=1}^{n_i} L_b(t_j^i - t_l) \int_{t_{j-1}^i}^{t_j^i} (X_{i,t_j^i} - X_{i,s}) ds, \\ \Pi_{i,l}(3) &= \sum_{j=1}^{n_i} \int_{t_{j-1}^i}^{t_j^i} [L_b(t_j^i - t_l) - L_b(s - t_l)] X_{i,s} ds, \\ \Pi_{i,l}(4) &= \int_0^{T_i} L_b(s - t_l) X_{i,s} ds - X_{i,t_i}, \quad T_i = t_{n_i}^i. \end{aligned}$$

We first use a truncation technique and the Bernstein-type inequality to show

$$P \left(\bigcup_{i=1}^p \left\{ \max_{1 \leq l \leq N} |\Pi_{i,l}(1)| > \frac{c_1^\dagger}{4} v_1(p, b, n_i) \right\} \right) \rightarrow 0, \quad \text{as } p, \underline{n} \rightarrow \infty, \quad (\text{A.2})$$

where c_{\dagger} is a sufficiently large positive constant and

$$\nu_1(p, b, n_i) = \left[\log(p \vee n_i) / (n_i^{2\beta_i+1} b) \right]^{1/2}.$$

Define $\varepsilon_{i,j}^* = \varepsilon_{i,j}^* \mathbf{I}(|\varepsilon_{i,j}^*| \leq n_i^{\kappa_1})$ and $\varepsilon_{i,j}^\diamond = \varepsilon_{i,j}^* \mathbf{I}(|\varepsilon_{i,j}^*| > n_i^{\kappa_1})$, where κ_1 is defined in Assumption 3(ii). Note that

$$\begin{aligned} \Pi_{i,l}(1) &= n_i^{-\beta_i} \sum_{j=1}^{n_i} L_b(t_j^i - t_l) \chi_i(t_j^i) (t_j^i - t_{j-1}^i) [\varepsilon_{i,j}^* - \mathbf{E}(\varepsilon_{i,j}^*)] + \\ &\quad n_i^{-\beta_i} \sum_{j=1}^{n_i} L_b(t_j^i - t_l) \chi_i(t_j^i) (t_j^i - t_{j-1}^i) [\varepsilon_{i,j}^\diamond - \mathbf{E}(\varepsilon_{i,j}^\diamond)]. \end{aligned}$$

By Assumption 2, we can prove that

$$\max_{1 \leq j \leq n_i} \mathbf{E}(|\chi_i(t_j^i) \varepsilon_{i,j}^\diamond|) = O(n_i^{-C_o}) = o(\nu_1(p, b, n_i)), \quad (\text{A.3})$$

where C_o is an arbitrarily large positive number. As

$$\max_{1 \leq i \leq p} \max_{1 \leq l \leq N} \sum_{j=1}^{n_i} L_b(t_j^i - t_l) (t_j^i - t_{j-1}^i) = O(1), \quad (\text{A.4})$$

using (A.3), (3.4) in Assumption 2(i), (3.5) in Assumption 3(ii) and the Bonferroni and Markov inequalities, we have

$$\begin{aligned} &\mathbf{P} \left(\bigcup_{i=1}^p \left\{ \max_{1 \leq l \leq N} \left| \sum_{j=1}^{n_i} L_b(t_j^i - t_l) \chi_i(t_j^i) (t_j^i - t_{j-1}^i) [\varepsilon_{i,j}^\diamond - \mathbf{E}(\varepsilon_{i,j}^\diamond)] \right| > \frac{c_{\dagger}}{8} n_i^{\beta_i} \nu_1(p, b, n_i) \right\} \right) \\ &\leq \mathbf{P} \left(\bigcup_{i=1}^p \left\{ \max_{1 \leq l \leq N} \left| \sum_{j=1}^{n_i} L_b(t_j^i - t_l) \chi_i(t_j^i) (t_j^i - t_{j-1}^i) \varepsilon_{i,j}^\diamond \right| > \frac{c_{\dagger}}{9} \nu_o(p, b, n_i) \right\} \right) \\ &\leq \mathbf{P} \left(\max_{1 \leq i \leq p} \max_{1 \leq j \leq n_i} |\varepsilon_{i,j}^\diamond| > 0 \right) \leq \mathbf{P} \left(\bigcup_{i=1}^p \left\{ \max_{1 \leq j \leq n_i} |\varepsilon_{i,j}^*| > n_i^{\kappa_1} \right\} \right) \\ &\leq \sum_{i=1}^p \sum_{j=1}^{n_i} \mathbf{P}(|\varepsilon_{i,j}^*| > n_i^{\kappa_1}) = O \left(\sum_{i=1}^p n_i \exp\{-s_0 n_i^{\kappa_1}\} \right) = o(1), \end{aligned} \quad (\text{A.5})$$

where s_0 is defined in (3.4) and

$$\nu_o(p, b, n_i) = \left[\frac{\log(p \vee n_i)}{n_i b} \right]^{1/2}.$$

On the other hand, by Assumptions 2 and 4(i) as well as the Bernstein inequality in Lemma B.1, we may show that

$$\begin{aligned} & \mathbb{P} \left(\bigcup_{i=1}^p \left\{ \max_{1 \leq l \leq N} \left| \sum_{j=1}^{n_i} L_b(t_j^i - t_l) \chi_i(t_j^i) (t_j^i - t_{j-1}^i) [\varepsilon_{i,j}^* - \mathbb{E}(\varepsilon_{i,j}^*)] \right| > \frac{c_{\dagger}}{8} n_i^{\beta_i} \nu_1(p, b, n_i) \right\} \right) \\ & \leq \sum_{i=1}^p \sum_{l=1}^N \mathbb{P} \left(\left| \sum_{j=1}^{n_i} L_b(t_j^i - t_l) \chi_i(t_j^i) (t_j^i - t_{j-1}^i) [\varepsilon_{i,j}^* - \mathbb{E}(\varepsilon_{i,j}^*)] \right| > \frac{c_{\dagger}}{8} \nu_o(p, b, n_i) \right) \\ & = O \left(N \sum_{i=1}^p \exp \{ -C_1 c_{\dagger}^2 \log(p \vee n_i) \} + N \sum_{i=1}^p \phi_i \exp \left\{ \frac{\log \gamma_0}{n_i^{\kappa_1} \cdot \nu_o(p, b, n_i)} \right\} \right), \end{aligned} \quad (\text{A.6})$$

where C_1 is a positive and bounded constant, $\gamma_0 \in (0, 1)$ is defined in Assumption 2(i) and $\phi_i = (n_i/b)^{3/4} n_i^{3\kappa_1/2} [\log(p \vee n_i)]^{1/4}$. By Assumption 3(i), letting $c_{\dagger} > 0$ be sufficiently large in (A.6), we have

$$N \sum_{i=1}^p \exp \{ -C_1 c_{\dagger}^2 \log(p \vee n_i) \} = o(1). \quad (\text{A.7})$$

Since $[\nu_o(p, b, n_i) n_i^{2\kappa_1}]^{-1} \rightarrow \infty$ for any i by the first condition in (3.5), and $N\phi_i$ diverges to infinity at a polynomial rate of n_i , we may show that

$$N \sum_{i=1}^p \phi_i \exp \left\{ \frac{\log \gamma_0}{n_i^{\kappa_1} \nu_o(p, b, n_i)} \right\} = o \left(\sum_{i=1}^p n_i \exp \{ -s_0 n_i^{\kappa_1} \} \right) = o(1). \quad (\text{A.8})$$

By (A.6)–(A.8), we have

$$\mathbb{P} \left(\bigcup_{i=1}^p \left\{ \max_{1 \leq l \leq N} \left| \sum_{j=1}^{n_i} L_b(t_j^i - t_l) \chi_i(t_j^i) (t_j^i - t_{j-1}^i) [\varepsilon_{i,j}^* - \mathbb{E}(\varepsilon_{i,j}^*)] \right| > \frac{c_{\dagger}}{8} n_i^{\beta_i} \nu_1(p, b, n_i) \right\} \right) = o(1), \quad (\text{A.9})$$

as p and \underline{n} jointly diverge to infinity. By (A.5) and (A.9), we prove (A.2).

Letting

$$\nu_2(p, b, n_i) = \sqrt{b \log(p \vee n_i)},$$

we next show that

$$\mathbf{P} \left(\bigcup_{i=1}^p \left\{ \max_{1 \leq l \leq n} |\Pi_{i,l}(2)| > \frac{c_{\dagger}}{4} \nu_2(p, b, n_i) \right\} \right) \rightarrow 0, \text{ as } p, \underline{n} \rightarrow \infty. \quad (\text{A.10})$$

By (1.2), (2.3) and (2.4), we decompose $\Pi_{i,l}(2)$ as

$$\begin{aligned} \Pi_{i,l}(2) &= \sum_{j=1}^{n_i} L_b(t_k - t_l) \int_{t_{j-1}^i}^{t_j^i} \left[\int_s^{t_j^i} (\Lambda_i(t)^\top \mu_t^F + \mu_{i,t}^U) dt \right] ds + \\ &\quad \sum_{j=1}^{n_i} L_b(t_k - t_l) \int_{t_{j-1}^i}^{t_j^i} \left[\int_s^{t_j^i} (\Lambda_i(t)^\top dW_t^F + (\sigma_{i,\bullet,t}^U)^\top dW_t^U) \right] ds \\ &=: \Pi_{i,l}(2, 1) + \Pi_{i,l}(2, 2), \end{aligned}$$

where $\sigma_{i,\bullet,t}^U = (\sigma_{i1,t}^U, \dots, \sigma_{ip,t}^U)^\top$. Let \mathcal{B} denote the event that (3.8)–(3.10) hold, and \mathcal{B}^c be the complement of \mathcal{B} . It follows from Assumption 4(i) that

$$\left\{ \max_{1 \leq l \leq n} |\Pi_{i,l}(2, 1)| > \frac{c_{\dagger}}{8} \nu_2(p, b, n_i) \right\}$$

is empty for all $i = 1, \dots, p$, conditional on \mathcal{B} . As $\mathbf{P}(\mathcal{B}^c) \rightarrow 0$, we readily have that

$$\mathbf{P} \left(\bigcup_{i=1}^p \left\{ \max_{1 \leq l \leq N} |\Pi_{i,l}(2, 1)| > \frac{c_{\dagger}}{8} \nu_2(p, b, n_i) \right\} \right) \rightarrow 0. \quad (\text{A.11})$$

By the Bonferroni inequality, we may show that, for any $\epsilon > 0$,

$$\begin{aligned} &\mathbf{P} \left(\bigcup_{i=1}^p \left\{ \max_{1 \leq j \leq n_i} \sup_{t_{j-1}^i \leq s \leq t_j^i} \left| \int_s^{t_j^i} (\Lambda_i(t)^\top dW_t^F + (\sigma_{i,\bullet,t}^U)^\top dW_t^U) \right| > \epsilon \nu_2(p, b, n_i) \right\} \right) \\ &\leq \sum_{i=1}^p \sum_{j=1}^{n_i} \mathbf{P} \left(\sup_{t_{j-1}^i \leq s \leq t_j^i} \left| \int_s^{t_j^i} (\Lambda_i(t)^\top dW_t^F + (\sigma_{i,\bullet,t}^U)^\top dW_t^U) \right| > \epsilon \nu_2(p, b, n_i) \right) \\ &\leq \sum_{i=1}^p \sum_{j=1}^{n_i} \mathbf{P} \left(\sup_{t_{j-1}^i \leq s \leq t_j^i} \left| \int_{t_{j-1}^i}^s (\Lambda_i(t)^\top dW_t^F + (\sigma_{i,\bullet,t}^U)^\top dW_t^U) \right| > \frac{\epsilon}{2} \nu_2(p, b, n_i) \right). \quad (\text{A.12}) \end{aligned}$$

Note that

$$\left\{ \left| \int_{t_{j-1}^i}^s (\Lambda_i(t)^\top dW_t^F + (\sigma_{i,\bullet,t}^U)^\top dW_t^U) \right| : s \geq t_{j-1}^i \right\}$$

and

$$\left\{ \exp \left(\psi \left| \int_{t_{j-1}^i}^s \left(\Lambda_i(t)^\top dW_t^F + (\sigma_{i,\bullet,t}^U)^\top dW_t^U \right) \right| \right) : s \geq t_{j-1}^i \right\} \text{ with } \psi > 0$$

are sub-martingales, which can be verified via the conditional Jensen inequality. Using the moment generating function for the folded normal random variable and Assumptions 1(ii)(iii) and 3(i), we can prove that

$$\mathbb{E} \left[\exp \left(\psi \left| \int_{t_{j-1}^i}^{t_j^i} \left(\Lambda_i(t)^\top dW_t^F + (\sigma_{i,\bullet,t}^U)^\top dW_t^U \right) \right| \right) \right] \leq \exp \left\{ \frac{\psi^2 c_j^i C_2}{2n_i} \right\}, \quad (\text{A.13})$$

where

$$C_2 = \max_{1 \leq i \leq p} \sup_{0 \leq t \leq T_i} [\Lambda_i(t)^\top \Lambda_i(t) + \sigma_{U,ii}(t)] < \infty.$$

By (A.13) and Doob's inequality for sub-martingales, we have

$$\begin{aligned} & \mathbb{P} \left(\sup_{t_{j-1}^i \leq s \leq t_j^i} \left| \int_{t_{j-1}^i}^s \left(\Lambda_i(t)^\top dW_t^F + (\sigma_{i,\bullet,t}^U)^\top dW_t^U \right) \right| > \frac{\epsilon}{2} \nu_2(p, b, n_i) \right) \\ &= \mathbb{P} \left(\sup_{t_{j-1}^i \leq s \leq t_j^i} \exp \left\{ \psi \left| \int_{t_{j-1}^i}^s \left(\Lambda_i(t)^\top dW_t^F + (\sigma_{i,\bullet,t}^U)^\top dW_t^U \right) \right| \right\} > \exp \left\{ \frac{\psi \epsilon \nu_2(p, b, n_i)}{2} \right\} \right) \\ &\leq \exp \left(-\frac{\psi \epsilon \nu_2(p, b, n_i)}{2} \right) \mathbb{E} \left[\exp \left(\psi \left| \int_{t_{j-1}^i}^{t_j^i} \left(\Lambda_i(t)^\top dW_t^F + (\sigma_{i,\bullet,t}^U)^\top dW_t^U \right) \right| \right) \right] \\ &\leq \exp \left\{ \frac{\psi^2 c_j^i C_2}{2n_i} - \frac{\psi \epsilon \nu_2(p, b, n_i)}{2} \right\}. \end{aligned} \quad (\text{A.14})$$

Then, choosing $\psi = \psi_j^i = \epsilon \nu_2(p, b, n_i) n_i / (2c_j^i C_2)$ in (A.14), by (A.12), (A.14) and Assumption 3, we have

$$\begin{aligned} & \mathbb{P} \left(\bigcup_{i=1}^p \left\{ \max_{1 \leq j \leq n_i} \sup_{t_{j-1}^i \leq s \leq t_j^i} \left| \int_s^{t_j^i} \left(\Lambda_i(t)^\top dW_t^F + (\sigma_{i,\bullet,t}^U)^\top dW_t^U \right) \right| > \epsilon \nu_2(p, b, n_i) \right\} \right) \\ &\leq \sum_{i=1}^p n_i \exp \left\{ -\frac{\epsilon^2}{8\bar{c}C_2} (n_i b) \log(p \vee n_i) \right\} = o(1), \end{aligned} \quad (\text{A.15})$$

where \bar{c} is defined in Assumption 3(i). This, together with (A.4), indicates that

$$\mathbb{P} \left(\bigcup_{i=1}^p \left\{ \max_{1 \leq l \leq N} |\Pi_{i,l}(2, 2)| > \frac{c_\dagger}{8} \nu_2(p, b, n_i) \right\} \right) \rightarrow 0, \text{ as } p, \underline{n} \rightarrow \infty. \quad (\text{A.16})$$

Combining (A.11) and (A.16), we prove (A.10).

We next prove that

$$\mathbf{P} \left(\bigcup_{i=1}^p \left\{ \max_{1 \leq l \leq N} |\Pi_{i,l}(3)| > \frac{c_{\dagger}}{4} \nu_3(p, b, n_i) \right\} \right) \rightarrow 0, \text{ as } p, \underline{n} \rightarrow \infty, \quad (\text{A.17})$$

where

$$\nu_3(p, b, n_i) = (n_i b)^{-1} \sqrt{\log(p \vee n_i)}.$$

Note that

$$|\Pi_{i,l}(3)| \leq \sup_{0 \leq t \leq T_i} |X_{i,t}| \cdot \sum_{j=1}^{n_i} \int_{t_{j-1}^i}^{t_j^i} |L_b(t_j^i - t_l) - L_b(s - t_l)| ds,$$

where $T_i = t_{n_i}^i$ is fixed. By the conditions on the kernel function $L(\cdot)$ in Assumption 4(i), we have

$$\max_{1 \leq l \leq n} \sum_{j=1}^{n_i} \int_{t_{j-1}^i}^{t_j^i} |L_b(t_j^i - t_l) - L_b(s - t_l)| ds = O((n_i b)^{-1}). \quad (\text{A.18})$$

On the other hand, by (3.8) and (3.10),

$$\sup_{0 \leq t \leq T_i} |X_{i,t}| \leq \sup_{0 \leq t \leq T_i} \left| \int_0^t \left[\Lambda_i(s)^\top dW_s^F + (\sigma_{i\bullet,s}^u)^\top dW_s^u \right] \right| + (C_\mu + k^{1/2} C_\mu C_\Lambda) T.$$

Following the proof of (A.15), we may show that, for $c_{\dagger} > 0$ large enough,

$$\mathbf{P} \left(\bigcup_{i=1}^p \left\{ \sup_{0 \leq t \leq T_i} \left| \int_0^t \left[\Lambda_i(s)^\top dW_s^F + (\sigma_{i\bullet,s}^u)^\top dW_s^u \right] \right| > c_{\dagger} \sqrt{\log(p \vee n_i)} \right\} \right) \rightarrow 0, \text{ as } p, \underline{n} \rightarrow \infty,$$

indicating that

$$\mathbf{P} \left(\bigcup_{i=1}^p \left\{ \sup_{0 \leq t \leq T_i} |X_{i,t}| > 2c_{\dagger} \sqrt{\log(p \vee n_i)} \right\} \right) \rightarrow 0, \text{ as } p, \underline{n} \rightarrow \infty. \quad (\text{A.19})$$

By virtue of (A.18) and (A.19), we complete the proof of (A.17) when c_{\dagger} is sufficiently large.

Finally, we consider $\Pi_{i,l}(4)$. Note that

$$\begin{aligned} \Pi_{i,l}(4) &= \left\{ \int_0^{T_i} L_b(s - t_l) \left[\int_0^s (\Lambda_i(t)^\top \mu_t^F + \mu_{i,t}^u) dt \right] ds - \int_0^{t_l} (\Lambda_i(t)^\top \mu_{i,t}^F + \mu_{i,t}^u) dt \right\} + \\ &\quad \left\{ \int_0^{T_i} L_b(s - t_l) \left[\int_0^s \left(\Lambda_i(t)^\top dW_t^F + (\sigma_{i\bullet,t}^u)^\top dW_t^u \right) \right] ds - \right. \end{aligned}$$

$$\int_0^{t_1} \left(\Lambda_i(t)^\top dW_t^F + (\sigma_{i\bullet,t}^U)^\top dW_t^U \right) \Big\} \\ =: \Pi_{i,1}(4,1) + \Pi_{i,1}(4,2).$$

With Assumption 4(i), (3.8) and (3.10), we have

$$\max_{1 \leq i \leq p} \max_{1 \leq l \leq N} |\Pi_{i,l}(4,1)| = O_p(b). \quad (\text{A.20})$$

Following the proof of (A.15), we may show that

$$\mathbb{P} \left(\bigcup_{i=1}^p \left\{ \max_{1 \leq l \leq N} \sup_{t_l \leq s \leq t_l+b} \left| \int_{t_l}^s \left(\Lambda_i(t)^\top dW_t^F + (\sigma_{i\bullet,t}^U)^\top dW_t^U \right) \right| > \frac{c_\dagger}{6} \nu_2(p, b, n_i) \right\} \right) \rightarrow 0$$

and

$$\mathbb{P} \left(\bigcup_{i=1}^p \left\{ \max_{1 \leq l \leq N} \sup_{t_l-b \leq s \leq t_l} \left| \int_s^{t_l} \left(\Lambda_i(t)^\top dW_t^F + (\sigma_{i\bullet,t}^U)^\top dW_t^U \right) \right| > \frac{c_\dagger}{6} \nu_2(p, b, n_i) \right\} \right) \rightarrow 0$$

as $p, \underline{n} \rightarrow \infty$ and $c_\dagger > 0$ is large enough. Consequently, we have

$$\mathbb{P} \left(\bigcup_{i=1}^p \left\{ \max_{1 \leq l \leq N} |\Pi_{i,l}(4,2)| > \frac{c_\dagger}{3} \nu_2(p, b, n_i) \right\} \right) \rightarrow 0. \quad (\text{A.21})$$

By virtue of (A.20) and (A.21), noting that $b/\nu_2(p, b, n_i) \rightarrow 0$, we can prove that

$$\mathbb{P} \left(\bigcup_{i=1}^p \left\{ \max_{1 \leq l \leq N} |\Pi_{i,l}(4)| > \frac{c_\dagger}{2} \nu_2(p, b, n_i) \right\} \right) \rightarrow 0, \text{ as } p, \underline{n} \rightarrow \infty. \quad (\text{A.22})$$

The proof of Proposition 3.1 is completed with (A.2), (A.10), (A.17) and (A.22). ■

A.2 Proof of Theorem 3.1

By the property of the shrinkage function, we have

$$\begin{aligned} & \sup_{h \leq \tau \leq T-h} \left\| \widehat{\Sigma}_U(\tau) - \Sigma_U(\tau) \right\|_{\max} \\ &= \max_{1 \leq i_1 \leq p} \max_{1 \leq i_2 \leq p} \sup_{h \leq \tau \leq T-h} |\widehat{\sigma}_{U,i_1 i_2}(\tau) - \sigma_{U,i_1 i_2}(\tau)| \\ &\leq \max_{1 \leq i_1 \leq p} \max_{1 \leq i_2 \leq p} \sup_{h \leq \tau \leq T-h} |\check{\sigma}_{U,i_1 i_2}(\tau) - \sigma_{U,i_1 i_2}(\tau)| + \sup_{0 \leq \tau \leq T} \rho(\tau). \end{aligned}$$

By Assumption 4(iii), in order to prove (3.13), it is sufficient to show that

$$\max_{1 \leq i_1 \leq p} \max_{1 \leq i_2 \leq p} \sup_{h \leq \tau \leq T-h} |\check{\sigma}_{\mathbf{U}, i_1 i_2}(\tau) - \sigma_{\mathbf{U}, i_1 i_2}(\tau)| = O_P(\zeta(p, b, h, \mathbf{n}, N)). \quad (\text{A.23})$$

Write $\mathbf{U}_j(\tau) = [\mathbf{U}_{1,j}(\tau), \dots, \mathbf{U}_{p,j}(\tau)]^\top = \Delta \mathbf{U}_j \mathbf{K}_h^{1/2}(\mathbf{t}_j - \tau)$. Note that

$$\begin{aligned} \check{\sigma}_{\mathbf{U}, i_1 i_2}(\tau) &= \sum_{j=1}^N \tilde{\mathbf{U}}_{i_1, j}(\tau) \tilde{\mathbf{U}}_{i_2, j}(\tau) \\ &= \sum_{j=1}^N \mathbf{U}_{i_1, j}(\tau) \mathbf{U}_{i_2, j}(\tau) + \sum_{j=1}^N [\tilde{\mathbf{U}}_{i_1, j}(\tau) - \mathbf{U}_{i_1, j}(\tau)] \mathbf{U}_{i_2, j}(\tau) + \\ &\quad \sum_{j=1}^N \mathbf{U}_{i_1, j}(\tau) [\tilde{\mathbf{U}}_{i_2, j}(\tau) - \mathbf{U}_{i_2, j}(\tau)] + \sum_{j=1}^N [\tilde{\mathbf{U}}_{i_1, j}(\tau) - \mathbf{U}_{i_1, j}(\tau)] [\tilde{\mathbf{U}}_{i_2, j}(\tau) - \mathbf{U}_{i_2, j}(\tau)]. \end{aligned} \quad (\text{A.24})$$

Following the proof of Proposition A.1 in [Bu et al. \(2023\)](#), we may show that

$$\max_{1 \leq i_1 \leq p} \max_{1 \leq i_2 \leq p} \sup_{h \leq \tau \leq T-h} \left| \sum_{j=1}^N \mathbf{U}_{i_1, j}(\tau) \mathbf{U}_{i_2, j}(\tau) - \sigma_{\mathbf{U}, i_1 i_2}(\tau) \right| = O_P \left(\left(\frac{\log(p \vee N)}{Nh} \right)^{1/2} + h^\delta \right). \quad (\text{A.25})$$

By (3.2) in Assumption 1(iii), (3.12) in Remark 3.2(i) and Lemmas [B.2–B.4](#) in Appendix B, we have

$$\max_{1 \leq i \leq p} \sup_{h \leq \tau \leq T-h} \sum_{j=1}^N [\tilde{\mathbf{U}}_{ij}(\tau) - \mathbf{U}_{ij}(\tau)]^2 = O_P([\zeta(p, b, h, \mathbf{n}, N)]^2). \quad (\text{A.26})$$

Combining (A.25), (A.26) and the Cauchy-Schwarz inequality, we can prove that

$$\max_{1 \leq i_1 \leq p} \max_{1 \leq i_2 \leq p} \sup_{h \leq \tau \leq T-h} \left| \sum_{j=1}^N [\tilde{\mathbf{U}}_{i_1, j}(\tau) - \mathbf{U}_{i_1, j}(\tau)] \mathbf{U}_{i_2, j}(\tau) \right| = O_P(\zeta(p, b, h, \mathbf{n}, N)), \quad (\text{A.27})$$

$$\max_{1 \leq i_1 \leq p} \max_{1 \leq i_2 \leq p} \sup_{h \leq \tau \leq T-h} \left| \sum_{j=1}^N \mathbf{U}_{i_1, j}(\tau) [\tilde{\mathbf{U}}_{i_2, j}(\tau) - \mathbf{U}_{i_2, j}(\tau)] \right| = O_P(\zeta(p, b, h, \mathbf{n}, N)), \quad (\text{A.28})$$

$$\begin{aligned} &\max_{1 \leq i_1 \leq p} \max_{1 \leq i_2 \leq p} \sup_{h \leq \tau \leq T-h} \left| \sum_{j=1}^N [\tilde{\mathbf{U}}_{i_1, j}(\tau) - \mathbf{U}_{i_1, j}(\tau)] [\tilde{\mathbf{U}}_{i_2, j}(\tau) - \mathbf{U}_{i_2, j}(\tau)] \right| \\ &= O_P([\zeta(p, b, h, \mathbf{n}, N)]^2) = o_P(\zeta(p, b, h, \mathbf{n}, N)). \end{aligned} \quad (\text{A.29})$$

By virtue of (A.25) and (A.27)–(A.29), we complete the proof of (A.23).

We next turn to the proof of (3.14). By the definition of shrinkage, we may show that

$$\begin{aligned}
& \sup_{h \leq \tau \leq T-h} \left\| \widehat{\Sigma}_U(\tau) - \Sigma_U(\tau) \right\|_s \\
& \leq \sup_{h \leq \tau \leq T-h} \max_{1 \leq i_1 \leq p} \sum_{i_2=1}^p |\widehat{\sigma}_{U,i_1 i_2}(\tau) - \sigma_{U,i_1 i_2}(\tau)| \\
& = \sup_{h \leq \tau \leq T-h} \max_{1 \leq i_1 \leq p} \sum_{i_2=1}^p |s_{\rho(\tau)}(\check{\sigma}_{U,i_1 i_2}(\tau)) I(|\check{\sigma}_{U,i_1 i_2}(\tau)| > \rho(\tau)) - \sigma_{U,i_1 i_2}(\tau)| \\
& \leq \sup_{h \leq \tau \leq T-h} \max_{1 \leq i_1 \leq p} \sum_{i_2=1}^p |s_{\rho(\tau)}(\check{\sigma}_{U,i_1 i_2}(\tau)) - \check{\sigma}_{U,i_1 i_2}(\tau)| I(|\check{\sigma}_{U,i_1 i_2}(\tau)| > \rho(\tau)) + \\
& \quad \sup_{h \leq \tau \leq T-h} \max_{1 \leq i_1 \leq p} \sum_{i_2=1}^p |\check{\sigma}_{U,i_1 i_2}(\tau) - \sigma_{U,i_1 i_2}(\tau)| I(|\check{\sigma}_{U,i_1 i_2}(\tau)| > \rho(\tau)) + \\
& \quad \sup_{h \leq \tau \leq T-h} \max_{1 \leq i_1 \leq p} \sum_{i_2=1}^p |\sigma_{U,i_1 i_2}(\tau)| I(|\check{\sigma}_{U,i_1 i_2}(\tau)| \leq \rho(\tau)) \\
& =: \Xi_1 + \Xi_2 + \Xi_3.
\end{aligned} \tag{A.30}$$

Define the event

$$\mathcal{M}(c) = \left\{ \max_{1 \leq i_1 \leq p} \max_{1 \leq i_2 \leq p} \sup_{h \leq \tau \leq T-h} |\check{\sigma}_{U,i_1 i_2}(\tau) - \sigma_{U,i_1 i_2}(\tau)| \leq c \cdot \zeta(p, b, h, \mathbf{n}, N) \right\},$$

where c is a positive constant. For any small $\epsilon > 0$, by (A.23), we may find $c_\epsilon > 0$ such that

$$\mathcal{P}(\mathcal{M}(c_\epsilon)) \geq 1 - \epsilon. \tag{A.31}$$

As $\{\Sigma_U(t) : 0 \leq t \leq T\} \in \mathcal{S}(q, \varpi_p)$, by Assumption 4(iii) with $\underline{C}_M \geq 2c_\epsilon$ and property (iii) of the shrinkage function, we may show that

$$\begin{aligned}
\Xi_1 + \Xi_2 & \leq (\bar{C}_M + c_\epsilon) \zeta(p, b, h, \mathbf{n}, N) \left[\sup_{h \leq \tau \leq T-h} \max_{1 \leq i_1 \leq p} \sum_{i_2=1}^p I(|\check{\sigma}_{U,i_1 i_2}(\tau)| > \rho(\tau)) \right] \\
& \leq (\bar{C}_M + c_\epsilon) \zeta(p, b, h, \mathbf{n}, N) \left[\sup_{h \leq \tau \leq T-h} \max_{1 \leq i_1 \leq p} \sum_{i_2=1}^p I(|\check{\sigma}_{U,i_1 i_2}(\tau)| > \underline{C}_M \zeta(p, b, h, \mathbf{n}, N)) \right] \\
& \leq (\bar{C}_M + c_\epsilon) \zeta(p, b, h, \mathbf{n}, N) \left[\sup_{h \leq \tau \leq T-h} \max_{1 \leq i_1 \leq p} \sum_{i_2=1}^p I(|\sigma_{U,i_1 i_2}(\tau)| > c_\epsilon \zeta(p, b, h, \mathbf{n}, N)) \right]
\end{aligned}$$

$$\begin{aligned}
&\leq C \cdot \zeta(p, b, h, \mathbf{n}, N) \left[\sup_{h \leq \tau \leq T-h} \max_{1 \leq i_1 \leq p} \sum_{i_2=1}^p \frac{|\sigma_{U, i_1 i_2}(\tau)|^q}{(c_\epsilon \zeta(p, b, h, \mathbf{n}, N))^q} \right] \\
&= O_p \left(\Psi \omega_p \zeta(p, b, h, \mathbf{n}, N)^{1-q} \right) = O_p \left(\omega_p \zeta(p, b, h, \mathbf{n}, N)^{1-q} \right)
\end{aligned} \tag{A.32}$$

on the event $\mathcal{M}(c_\epsilon)$.

On the other hand, we note that the events $\{|\check{\sigma}_{U, i_1 i_2}(\tau)| \leq \rho(\tau)\}$ and $\mathcal{M}(c_\epsilon)$ jointly imply that $\{|\sigma_{U, i_1 i_2}(\tau)| \leq (\bar{C}_M + c_\epsilon) \zeta(p, b, h, \mathbf{n}, N)\}$ by the triangle inequality. Then,

$$\begin{aligned}
\Xi_3 &\leq \sup_{h \leq \tau \leq T-h} \max_{1 \leq i_1 \leq p} \sum_{i_2=1}^p |\sigma_{U, i_1 i_2}(\tau)| I(|\sigma_{U, i_1 i_2}(\tau)| \leq (\bar{C}_M + c_\epsilon) \zeta(p, b, h, \mathbf{n}, N)) \\
&\leq (\bar{C}_M + c_\epsilon)^{1-q} \zeta(p, b, h, \mathbf{n}, N)^{1-q} \sup_{h \leq \tau \leq T-h} \max_{1 \leq i_1 \leq p} \sum_{i_2=1}^p |\sigma_{U, i_1 i_2}(\tau)|^q \\
&= O_p \left(\Psi \omega_p \zeta(p, b, h, \mathbf{n}, N)^{1-q} \right) \\
&= O_p \left(\omega_p \zeta(p, b, h, \mathbf{n}, N)^{1-q} \right).
\end{aligned} \tag{A.33}$$

By (A.32) and (A.33), letting $\epsilon \rightarrow 0$ in (A.31), we complete the proof of (3.14). \blacksquare

A.3 Proof of Theorem 3.2

Define

$$\Sigma_X^*(\tau) = \Lambda(\tau) \Sigma_F^*(\tau) \Lambda(\tau)^\top + \Sigma_U(\tau) \text{ with } \Sigma_F^*(\tau) = \Delta F(\tau)^\top \Delta F(\tau) = \sum_{t=1}^N \Delta F_t(\tau) \Delta F_t(\tau)^\top.$$

Observe that

$$\begin{aligned}
&\sup_{h \leq \tau \leq T-h} \left\| \hat{\Sigma}_X(\tau) - \Sigma_X(\tau) \right\|_{\max} \\
&\leq \sup_{h \leq \tau \leq T-h} \left\| \hat{\Sigma}_X(\tau) - \Sigma_X^*(\tau) \right\|_{\max} + \sup_{h \leq \tau \leq T-h} \left\| \Sigma_X^*(\tau) - \Sigma_X(\tau) \right\|_{\max},
\end{aligned}$$

and

$$\begin{aligned}
&\sup_{h \leq \tau \leq T-h} \left\| \hat{\Sigma}_X(\tau) - \Sigma_X^*(\tau) \right\|_{\max} \\
&\leq \sup_{h \leq \tau \leq T-h} \left[\left\| \hat{\Sigma}_U(\tau) - \Sigma_U(\tau) \right\|_{\max} + \left\| \tilde{\Lambda}(\tau) \tilde{\Lambda}(\tau)^\top - \Lambda(\tau) \Sigma_F^*(\tau) \Lambda(\tau)^\top \right\|_{\max} \right].
\end{aligned}$$

Let $\tilde{\Sigma}_F(\tau) = \sum_{t=1}^N \Delta \tilde{F}_t(\tau) \Delta \tilde{F}_t(\tau)^\top$. By Lemmas B.2 and B.4 in Appendix B, we have

$$\begin{aligned} & \sup_{h \leq \tau \leq T-h} \left\| \tilde{\Lambda}(\tau) \tilde{\Lambda}(\tau)^\top - \Lambda(\tau) \Sigma_F^*(\tau) \Lambda(\tau)^\top \right\|_{\max} \\ &= \sup_{h \leq \tau \leq T-h} \left\| \tilde{\Lambda}(\tau) \tilde{\Sigma}_F(\tau) \tilde{\Lambda}(\tau)^\top - \Lambda(\tau) \Sigma_F^*(\tau) \Lambda(\tau)^\top \right\|_{\max} \\ &= O_P(\zeta(p, b, h, \mathbf{n}, N)), \end{aligned}$$

which, together with (3.13) in Theorem 3.1, leads to

$$\sup_{h \leq \tau \leq T-h} \left\| \hat{\Sigma}_X(\tau) - \Sigma_X^*(\tau) \right\|_{\max} = O_P(\zeta(p, b, h, \mathbf{n}, N)). \quad (\text{A.34})$$

Due to the identification condition of $\Sigma_F(\tau) = \sigma_\tau^F(\sigma_\tau^F)^\top = I_k$, we may also show that

$$\sup_{h \leq \tau \leq T-h} \left\| \Sigma_X^*(\tau) - \Sigma_X(\tau) \right\|_{\max} = O_P \left(\left(\frac{\log(p \vee N)}{Nh} \right)^{1/2} + h^\delta \right). \quad (\text{A.35})$$

The proof of (3.16) is completed by virtue of (A.34) and (A.35).

We next turn to the proof of (3.17). For any $p \times p$ matrix Σ , we have

$$\|\Sigma\|_{\Sigma_X(\tau)}^2 = \frac{1}{p} \|\Sigma_X^{-1/2}(\tau) \Sigma \Sigma_X^{-1/2}(\tau)\|_F^2 \leq \frac{C}{p} \|\Sigma\|_F^2, \quad (\text{A.36})$$

since all the eigenvalues of $\Sigma_X(\tau)$ are positive and bounded away from 0. Note that

$$\begin{aligned} & \sup_{h \leq \tau \leq T-h} \left\| \hat{\Sigma}_X(\tau) - \Sigma_X(\tau) \right\|_{\Sigma_X(\tau)}^2 \\ & \leq C \sup_{h \leq \tau \leq T-h} \left[\left\| \hat{\Sigma}_X(\tau) - \Sigma_X^*(\tau) \right\|_{\Sigma_X(\tau)}^2 + \left\| \Sigma_X^*(\tau) - \Sigma_X(\tau) \right\|_{\Sigma_X(\tau)}^2 \right], \end{aligned}$$

where

$$\begin{aligned} & \sup_{h \leq \tau \leq T-h} \left\| \hat{\Sigma}_X(\tau) - \Sigma_X^*(\tau) \right\|_{\Sigma_X(\tau)}^2 \\ & \leq C \sup_{h \leq \tau \leq T-h} \left[\left\| \hat{\Sigma}_U(\tau) - \Sigma_U(\tau) \right\|_{\Sigma_X(\tau)}^2 + \left\| \tilde{\Lambda}(\tau) \tilde{\Lambda}(\tau)^\top - \Lambda(\tau) \Sigma_F^*(\tau) \Lambda(\tau)^\top \right\|_{\Sigma_X(\tau)}^2 \right]. \end{aligned}$$

By (A.36) and (3.14) in Theorem 3.1, we can prove that

$$\sup_{h \leq \tau \leq T-h} \left\| \hat{\Sigma}_U(\tau) - \Sigma_U(\tau) \right\|_{\Sigma_X(\tau)}^2$$

$$\begin{aligned}
&\leq \frac{C}{p} \sup_{h \leq \tau \leq T-h} \left\| \widehat{\Sigma}_U(\tau) - \Sigma_U(\tau) \right\|_F^2 \\
&\leq C \sup_{h \leq \tau \leq T-h} \left\| \widehat{\Sigma}_U(\tau) - \Sigma_U(\tau) \right\|_s^2 \\
&= O_p \left(\omega_p^2 [\zeta(p, b, h, \mathbf{n}, N)]^{2-2q} \right). \tag{A.37}
\end{aligned}$$

Let $D_\Lambda(\tau) = \widetilde{\Lambda}(\tau) - \Lambda(\tau)H_*(\tau)$, where $H_*(\tau) = [H(\tau)]^{-1}$ and $H(\tau)$ is a $k \times k$ rotation matrix defined as in Lemma B.2. Note that

$$\begin{aligned}
&\widetilde{\Lambda}(\tau)\widetilde{\Lambda}(\tau)^\top - \Lambda(\tau)\Sigma_F^*(\tau)\Lambda(\tau)^\top \\
&= D_\Lambda(\tau)D_\Lambda(\tau)^\top + D_\Lambda(\tau)H_*(\tau)^\top\Lambda(\tau)^\top + \Lambda(\tau)H_*(\tau)D_\Lambda(\tau)^\top + \\
&\Lambda(\tau) [H_*(\tau)H_*(\tau)^\top - \Sigma_F^*(\tau)] \Lambda(\tau)^\top.
\end{aligned}$$

By (A.36) and Lemma B.4, we have

$$\begin{aligned}
\sup_{h \leq \tau \leq T-h} \left\| D_\Lambda(\tau)D_\Lambda(\tau)^\top \right\|_{\Sigma_X(\tau)}^2 &\leq C \sup_{h \leq \tau \leq T-h} \frac{1}{p} \|D_\Lambda(\tau)\|_F^4 \\
&= O_p \left(p [\zeta(p, b, h, \mathbf{n}, N)]^4 \right). \tag{A.38}
\end{aligned}$$

By (2.6) and Assumption 1(iii), we may show that

$$\sup_{h \leq \tau \leq T-h} \left\| \Lambda(\tau)^\top \Sigma_X^{-1}(\tau) \Lambda(\tau) \right\|_s = O_p(1), \tag{A.39}$$

whose proof is similar to the proof of Theorem 2 in Fan, Fan and Lv (2008). Then, by (A.39), Lemmas B.3 and B.4, following the proof of Lemma 13 in Fan, Liao and Mincheva (2013), we have

$$\begin{aligned}
&\sup_{h \leq \tau \leq T-h} \left\| \Lambda(\tau)H_*(\tau)D_\Lambda(\tau)^\top \right\|_{\Sigma_X(\tau)}^2 \\
&= \frac{1}{p} \sup_{h \leq \tau \leq T-h} \text{trace} \left\{ H_*(\tau)D_\Lambda(\tau)^\top \Sigma_X^{-1}(\tau)D_\Lambda(\tau)H_*(\tau)^\top \Lambda(\tau)^\top \Sigma_X^{-1}(\tau)\Lambda(\tau) \right\} \\
&\leq \frac{C}{p} \sup_{h \leq \tau \leq T-h} \|H_*(\tau)\|_s^2 \|D_\Lambda(\tau)\|_F^2 \\
&= O_p \left([\zeta(p, b, h, \mathbf{n}, N)]^2 \right). \tag{A.40}
\end{aligned}$$

Similarly, we can also prove that

$$\sup_{h \leq \tau \leq T-h} \left\| D_\Lambda(\tau)H_*(\tau)^\top \Lambda(\tau)^\top \right\|_{\Sigma_X(\tau)}^2 = O_p \left([\zeta(p, b, h, \mathbf{n}, N)]^2 \right). \tag{A.41}$$

By Assumption 1(iii) and Lemmas B.2 and B.3, we may show that

$$\begin{aligned}
& \sup_{h \leq \tau \leq T-h} \left\| \Lambda(\tau) [H_*(\tau)H_*(\tau)^\top - \Sigma_F^*(\tau)] \Lambda(\tau)^\top \right\|_{\Sigma_X(\tau)}^2 \\
&= \sup_{h \leq \tau \leq T-h} \left\| \Lambda(\tau)H_*(\tau) \left[\sum_{t=1}^N \Delta \tilde{F}_t(\tau) \Delta \tilde{F}_t(\tau)^\top - \sum_{t=1}^N H(\tau) \Delta F_t(\tau) \Delta F_t(\tau)^\top H(\tau)^\top \right] H_*(\tau)^\top \Lambda(\tau)^\top \right\|_{\Sigma_X(\tau)}^2 \\
&\leq \frac{C}{p} \sup_{h \leq \tau \leq T-h} \left\| \sum_{t=1}^N \Delta \tilde{F}_t(\tau) \Delta \tilde{F}_t(\tau)^\top - \sum_{t=1}^N H(\tau) \Delta F_t(\tau) \Delta F_t(\tau)^\top H(\tau)^\top \right\|_F^2 \\
&= O_p \left(\frac{1}{p} [\zeta(p, b, h, \mathbf{n}, N)]^2 \right). \tag{A.42}
\end{aligned}$$

With (A.38), (A.40)–(A.42), we have

$$\begin{aligned}
& \sup_{h \leq \tau \leq T-h} \left\| \tilde{\Lambda}(\tau) \tilde{\Lambda}(\tau)^\top - \Lambda(\tau) \Sigma_F^*(\tau) \Lambda(\tau)^\top \right\|_{\Sigma_X(\tau)}^2 \\
&= O_p \left(p [\zeta(p, b, h, \mathbf{n}, N)]^4 + [\zeta(p, b, h, \mathbf{n}, N)]^2 \right). \tag{A.43}
\end{aligned}$$

Combining (A.37) and (A.43), indicates that

$$\begin{aligned}
& \sup_{h \leq \tau \leq T-h} \left\| \hat{\Sigma}_X(\tau) - \Sigma_X^*(\tau) \right\|_{\Sigma_X(\tau)}^2 \\
&= O_p \left(p [\zeta(p, b, h, \mathbf{n}, N)]^4 + \omega_p^2 [\zeta(p, b, h, \mathbf{n}, N)]^{2-2p} \right). \tag{A.44}
\end{aligned}$$

On the other hand, using (A.36) and following the proof of (A.42), we have

$$\begin{aligned}
\sup_{h \leq \tau \leq T-h} \left\| \Sigma_X^*(\tau) - \Sigma_X(\tau) \right\|_{\Sigma_X(\tau)}^2 &= O_p \left(\frac{1}{p} \left(\left(\frac{\log(p \vee N)}{Nh} \right)^{1/2} + h^\delta \right)^2 \right) \\
&= o_p \left([\zeta(p, b, h, \mathbf{n}, N)]^2 \right). \tag{A.45}
\end{aligned}$$

By virtue of (A.44) and (A.45), we complete the proof of (3.17). ■

B Technical lemmas and proofs

In this appendix, we provide some technical lemmas together with their proofs. As in Appendix A, we let C be a generic positive constant whose value may change from line to line. The first lemma is the Bernstein inequality for the α -mixing sequence (e.g., Bosq, 1998).

Lemma B.1. Let $\{Z_t, t \geq 1\}$ be a zero-mean α -mixing process satisfying $P(|Z_t| \leq B) = 1$ for all $t \geq 1$. Then, for each integer $q_1 \in [1, T/2]$ and each $\epsilon > 0$, we have

$$P\left(\left|\sum_{t=1}^T Z_t\right| > T\epsilon\right) \leq 4 \exp\left\{-\frac{\epsilon^2 q_1}{8\omega(q_1)}\right\} + 22\left(1 + \frac{4B}{\epsilon}\right)^{1/2} q_1 \alpha(\lfloor q_2 \rfloor), \quad (\text{B.1})$$

where $\omega(q_1) = 2\sigma^2(q_1)/q_2^2 + B\epsilon/2$, $q_2 = T/(2q_1)$,

$$\sigma^2(q_1) = \max_{1 \leq j \leq 2q_1-1} E \left\{ (\lfloor jq_2 \rfloor + 1 - jq_2) Z_{\lfloor jq_2 \rfloor + 1} + Z_{\lfloor jq_2 \rfloor + 2} + \cdots + Z_{\lfloor (j+1)q_2 \rfloor} \right. \\ \left. + ((j+1)q_2 - \lfloor (j+1)q_2 \rfloor) Z_{\lfloor (j+1)q_2 \rfloor + 1} \right\}^2,$$

$\alpha(\cdot)$ is the α -mixing coefficient and $\lfloor \cdot \rfloor$ denotes the floor function.

The following lemma derives the uniform mean square convergence rate of the local PCA estimates $\tilde{\Delta F}_t(\tau)$, $t = 1, \dots, N$, defined in Section 2.3. Define a $k \times k$ rotation matrix:

$$H(\tau) = [\tilde{V}(\tau)]^{-1} \left[\sum_{t=1}^N \tilde{\Delta F}_t(\tau) \Delta F_t(\tau)^\top \right] \left[\frac{1}{p} \Lambda(\tau)^\top \Lambda(\tau) \right],$$

where $\tilde{V}(\tau) = \text{diag}\{\tilde{v}_1(\tau), \dots, \tilde{v}_k(\tau)\}$ with $\tilde{v}_j(\tau)$ being the j -th largest eigenvalue of $\frac{1}{p} \Delta \tilde{X}(\tau)^\top \Delta \tilde{X}(\tau)$.

Lemma B.2. Suppose that Assumptions 1–3 and 4(i)(ii) are satisfied. Then, we have

$$\sup_{h \leq \tau \leq T-h} \sum_{t=1}^N \left\| \tilde{\Delta F}_t(\tau) - H(\tau) \Delta F_t(\tau) \right\|^2 = O_P\left([\zeta_o(p, b, h, \mathbf{n}, N)]^2\right), \quad (\text{B.2})$$

where

$$\zeta_o(p, b, h, \mathbf{n}, N) = \zeta_1(p, b, \mathbf{n}, N) + \zeta_2^\circ(p, h, N)$$

with $\zeta_1(p, b, \mathbf{n}, N)$ defined in Assumption 4(iii) and $\zeta_2^\circ(p, h, N) = \left(\frac{\omega_p}{ph}\right)^{1/2} + (Nh)^{-1/2} + h^\delta$.

Proof of Lemma B.2. By the definition of $\tilde{\Delta F}(\tau)$, we have

$$\frac{1}{p} \Delta \tilde{X}(\tau)^\top \Delta \tilde{X}(\tau) \tilde{\Delta F}(\tau) = \tilde{\Delta F}(\tau) \tilde{V}(\tau). \quad (\text{B.3})$$

Let $\Delta X_j = X_{t_j} - X_{t_{j-1}}$, $\Delta X_j(\tau) = \Delta X_j K_h^{1/2}(t_j - \tau)$, and $\tilde{\Delta X}_j(\tau)$ be the j -th column vector of $\Delta \tilde{X}(\tau)$. It follows from (B.3) that, for $j = 1, \dots, N$,

$$\tilde{V}(\tau) \tilde{\Delta F}_j(\tau) = \frac{1}{p} \sum_{s=1}^N \tilde{\Delta F}_s(\tau) \tilde{\Delta X}_s(\tau)^\top \tilde{\Delta X}_j(\tau)$$

$$\begin{aligned}
&= \frac{1}{p} \sum_{s=1}^N \Delta \tilde{F}_s(\tau) \Delta X_s(\tau)^\top \Delta X_j(\tau) + \\
&\quad \frac{1}{p} \sum_{s=1}^N \Delta \tilde{F}_s(\tau) \left[\Delta \tilde{X}_s(\tau) - \Delta X_s(\tau) \right]^\top \Delta X_j(\tau) + \\
&\quad \frac{1}{p} \sum_{s=1}^N \Delta \tilde{F}_s(\tau) \Delta \tilde{X}_s(\tau)^\top \left[\Delta \tilde{X}_j(\tau) - \Delta X_j(\tau) \right].
\end{aligned} \tag{B.4}$$

By (1.2) and (2.4), we write

$$\begin{aligned}
\Delta X_s(\tau) &= \left(\int_{t_{s-1}}^{t_s} \Lambda(t) dF_t \right) K_h^{1/2}(t_s - \tau) + \left(\int_{t_{s-1}}^{t_s} dU_t \right) K_h^{1/2}(t_s - \tau) \\
&= \left(\int_{t_{s-1}}^{t_s} \Lambda(t) dF_t \right) K_h^{1/2}(t_s - \tau) + \left(\int_{t_{s-1}}^{t_s} \mu_t^u dt \right) K_h^{1/2}(t_s - \tau) + \\
&\quad \left(\int_{t_{s-1}}^{t_s} \sigma_t^u dW_t^u \right) K_h^{1/2}(t_s - \tau) \\
&= R_{s,1}(\tau) + R_{s,2}(\tau) + R_{s,3}(\tau),
\end{aligned}$$

indicating that

$$\frac{1}{p} \sum_{s=1}^N \Delta \tilde{F}_s(\tau) \Delta X_s(\tau)^\top \Delta X_j(\tau) = \frac{1}{p} \sum_{l_1=1}^3 \sum_{l_2=1}^3 \sum_{s=1}^N \Delta \tilde{F}_s(\tau) R_{s,l_1}(\tau)^\top R_{j,l_2}(\tau). \tag{B.5}$$

By the smoothness restriction in Assumption 1(iii), we may show that

$$\begin{aligned}
&\frac{1}{p} \sum_{s=1}^N \Delta \tilde{F}_s(\tau) R_{s,1}(\tau)^\top R_{j,1}(\tau) \\
&= \left[\sum_{s=1}^N \Delta \tilde{F}_s(\tau) \Delta F_s(\tau)^\top \right] \left[\frac{1}{p} \Lambda(\tau)^\top \Lambda(\tau) \right] \Delta F_j(\tau) (1 + O_p(h^\delta)),
\end{aligned} \tag{B.6}$$

where δ is defined in Assumption 1(ii).

Following the argument in the proof of (A.14) with $v_2(p, b, n_i)$ and t_j^i replaced by $[N^{-1} \log(p \vee N)]^{1/2}$ and t_s , respectively, we can prove that

$$\max_{1 \leq i \leq p} \sup_{1 \leq s \leq n} |\Delta X_{i,s}| = O_p \left(\sqrt{N^{-1} \log(p \vee N)} \right), \tag{B.7}$$

where $\Delta X_{i,s}$ is the i -th component of ΔX_s . By (B.7), Assumption 1(i) and the Cauchy-Schwarz

inequality, and noting that

$$\sup_{h \leq \tau \leq T-h} \sum_{s=1}^N \left\| \Delta \tilde{F}_s(\tau) \right\|^2 = O_p(1) \quad (\text{B.8})$$

from the normalisation restriction (2.14), we have

$$\begin{aligned} & \sup_{h \leq \tau \leq T-h} \sum_{j=1}^N \left\| \frac{1}{p} \sum_{l_2=1}^3 \sum_{s=1}^N \Delta \tilde{F}_s(\tau) R_{s,2}(\tau)^\top R_{j,l_2}(\tau) \right\|^2 \\ &= \sup_{h \leq \tau \leq T-h} \sum_{j=1}^N \left\| \sum_{s=1}^N \Delta \tilde{F}_s(\tau) \frac{R_{s,2}(\tau)^\top \Delta X_j(\tau)}{p} \right\|^2 \\ &\leq \sup_{h \leq \tau \leq T-h} \sum_{s=1}^N \left\| \Delta \tilde{F}_s(\tau) \right\|^2 \sum_{j=1}^N \sum_{s=1}^N \left\| \frac{1}{p} R_{s,2}(\tau)^\top \Delta X_j(\tau) \right\|^2 \\ &= O_p \left(\frac{\log(p \vee N)}{N} \right), \end{aligned} \quad (\text{B.9})$$

and similarly

$$\sup_{h \leq \tau \leq T-h} \sum_{j=1}^N \left\| \frac{1}{p} \sum_{l_1=1}^3 \sum_{s=1}^N \Delta \tilde{F}_s(\tau) R_{s,l_1}(\tau)^\top R_{j,2}(\tau) \right\|^2 = O_p \left(\frac{\log(p \vee N)}{N} \right). \quad (\text{B.10})$$

Write

$$\begin{aligned} R_{s,1}(\tau) &= [\Lambda(t_{s-1}) \Delta F_s] K_h^{1/2}(t_s - \tau) + \left\{ \int_{t_{s-1}}^{t_s} [\Lambda(t) - \Lambda(t_{s-1})] dF_t \right\} K_h^{1/2}(t_s - \tau) \\ &=: R_{s,1}^*(\tau) + R_{s,1}^\diamond(\tau), \end{aligned}$$

and thus

$$\begin{aligned} & \sup_{h \leq \tau \leq T-h} \sum_{j=1}^N \left\| \frac{1}{p} \sum_{s=1}^N \Delta \tilde{F}_s(\tau) R_{s,1}(\tau)^\top R_{j,3}(\tau) \right\|^2 \\ &\leq 2 \sup_{h \leq \tau \leq T-h} \sum_{j=1}^N \left\| \frac{1}{p} \sum_{s=1}^N \Delta \tilde{F}_s(\tau) R_{s,1}^*(\tau)^\top R_{j,3}(\tau) \right\|^2 + \\ &\quad 2 \sup_{h \leq \tau \leq T-h} \sum_{j=1}^N \left\| \frac{1}{p} \sum_{s=1}^N \Delta \tilde{F}_s(\tau) R_{s,1}^\diamond(\tau)^\top R_{j,3}(\tau) \right\|^2. \end{aligned}$$

Write $R_{s,3}(\tau) = \mathbf{u}_s K_h^{1/2}(t_s - \tau)$ with $\mathbf{u}_s = (\mathbf{u}_{1,s}, \dots, \mathbf{u}_{p,s})^\top = \int_{t_{s-1}}^{t_s} \sigma_t^u dW_t^u$. Note that

$$\begin{aligned} & \sum_{j=1}^N \left\| \frac{1}{p} \sum_{s=1}^N \Delta \tilde{F}_s(\tau) R_{s,1}^*(\tau)^\top R_{j,3}(\tau) \right\|^2 \\ &= \sum_{j=1}^N \left\| \sum_{s=1}^N \Delta \tilde{F}_s(\tau) \Delta F_s(\tau)^\top \left[\frac{1}{p} \Lambda(t_{s-1})^\top \mathbf{u}_j \right] \right\|^2 K_h(t_j - \tau) \\ &\leq \left[\sum_{s=1}^N \|\Delta \tilde{F}_s(\tau)\|^2 \right] \left[\sum_{s=1}^N \|\Delta F_s(\tau)\|^2 \right] \left[\sum_{j=1}^N K_h(t_j - \tau) \right] \left[\max_{1 \leq s, j \leq n} \left\| \frac{1}{p} \Lambda(t_{s-1})^\top \mathbf{u}_j \right\|^2 \right]. \quad (\text{B.11}) \end{aligned}$$

By Proposition A.1 in [Bu et al. \(2023\)](#), we have

$$\sup_{h \leq \tau \leq T-h} \sum_{s=1}^N \|\Delta F_s(\tau)\|^2 = O_p(1). \quad (\text{B.12})$$

As in (A.13), using the moment generating function for the folded normal random variable, (2.6) and Assumption1(iii), for $l = 1, \dots, k$, we have

$$\mathbb{E} \left[\exp \left(\psi \left| \frac{1}{[p\varpi_p]^{1/2}} \sum_{i=1}^p \Lambda_{il}(t_{s-1}) \mathbf{u}_{i,j} \right| \right) \right] \leq \exp \left\{ \frac{\psi^2 \text{TC}_3}{2N} \right\},$$

where $\psi > 0$, $\Lambda_{il}(\cdot)$ is the (i, l) -entry of $\Lambda(\cdot)$, and

$$C_3 = \left[\max_{1 \leq i \leq p} \max_{1 \leq l \leq k} \sup_{0 \leq t \leq T} |\Lambda_{il}(t)|^2 \right] \left[\sup_{0 \leq t \leq T} \frac{1}{p\varpi_p} \sum_{1 \leq i_1, i_2 \leq p} \sigma_{\mathbf{u}, i_1 i_2}(t) \right]$$

is bounded with probability approaching one. This, together with the Markov inequality, leads to

$$\begin{aligned} & \mathbb{P} \left(\max_{1 \leq s \leq n} \max_{1 \leq j \leq N} \left| \frac{1}{p} \sum_{i=1}^p \Lambda_{il}(t_{s-1}) \mathbf{u}_{i,j} \right| > m \sqrt{\frac{\varpi_p \log N}{pN}} \right) \\ &= \mathbb{P} \left(\max_{1 \leq s \leq n} \max_{1 \leq j \leq N} \left| \frac{1}{(p\varpi_p)^{1/2}} \sum_{i=1}^p \Lambda_{il}(t_{s-1}) \mathbf{u}_{i,j} \right| > m \sqrt{\frac{\log N}{N}} \right) \\ &\leq \sum_{s=1}^N \sum_{j=1}^N \exp \left(-\psi m \sqrt{\frac{\log N}{N}} \right) \mathbb{E} \left[\exp \left(\psi \left| \frac{1}{(p\varpi_p)^{1/2}} \sum_{i=1}^p \Lambda_{il}(t_{s-1}) \mathbf{u}_{i,j} \right| \right) \right] \\ &\leq N^2 \exp \left\{ \frac{\psi^2 \text{TC}_3}{2N} - \psi m \sqrt{\frac{\log N}{N}} \right\}. \quad (\text{B.13}) \end{aligned}$$

Choosing $\psi = (mN \log N)^{1/2}$ and letting $m > 0$ be sufficiently large so that $m^{3/2} - (TmC_3)/2 > 2$ in (B.13), we have

$$\mathbb{P} \left(\max_{1 \leq s \leq n} \max_{1 \leq j \leq N} \left| \frac{1}{p} \sum_{i=1}^p \Lambda_{il}(t_{s-1}) u_{i,j} \right| > m \sqrt{\frac{\omega_p \log N}{pN}} \right) = o(N^2 \exp\{-2 \log N\}) = o(1)$$

for any $l = 1, \dots, k$, indicating that

$$\max_{1 \leq s \leq n} \max_{1 \leq j \leq N} \left\| \frac{\Lambda(t_{s-1})^\top u_j}{p} \right\|^2 = O_p \left(\frac{\omega_p \log N}{pN} \right). \quad (\text{B.14})$$

By (B.8), (B.11), (B.12), (B.14) and noting that $\frac{1}{N} \sum_{j=1}^N K_h(t_j - \tau) = O(1)$ uniformly over $h \leq \tau \leq T - h$, we can prove that

$$\sum_{j=1}^N \left\| \frac{1}{p} \sum_{s=1}^N \Delta \tilde{F}_s(\tau) R_{s,1}^*(\tau)^\top R_{j,3}(\tau) \right\|^2 = O_p \left(\frac{\omega_p \log N}{p} \right). \quad (\text{B.15})$$

On the other hand, by the Cauchy-Schwarz inequality, we have

$$\begin{aligned} & \sum_{j=1}^N \left\| \frac{1}{p} \sum_{s=1}^N \Delta \tilde{F}_s(\tau) R_{s,1}^\diamond(\tau)^\top R_{j,3}(\tau) \right\|^2 \\ & \leq \left[\sum_{s=1}^N \left\| \Delta \tilde{F}_s(\tau) \right\|^2 \right] \left[\sum_{s=1}^N \frac{1}{p} \left\| \int_{t_{s-1}}^{t_s} [\Lambda(t) - \Lambda(t_{s-1})] dF_t \right\|^2 K_h(t_s - \tau) \right] \left[\frac{1}{p} \sum_{j=1}^N \|u_j\|^2 K_h(t_j - \tau) \right]. \end{aligned}$$

By Proposition A.1 in Bu *et al.* (2023) and the smoothness condition (3.2), we may show that

$$\sup_{h \leq \tau \leq T-h} \frac{1}{p} \sum_{s=1}^N \left\| \int_{t_{s-1}}^{t_s} [\Lambda(t) - \Lambda(t_{s-1})] dF_t \right\|^2 K_h(t_s - \tau) = O_p(N^{-2\delta}), \quad (\text{B.16})$$

$$\sup_{h \leq \tau \leq T-h} \frac{1}{p} \sum_{j=1}^N \|u_j\|^2 K_h(t_j - \tau) = O_p(1). \quad (\text{B.17})$$

By (B.8), (B.16) and (B.17), we have

$$\sup_{h \leq \tau \leq T-h} \sum_{j=1}^N \left\| \frac{1}{p} \sum_{s=1}^N \Delta \tilde{F}_s(\tau) R_{s,1}^\diamond(\tau)^\top R_{j,3}(\tau) \right\|^2 = O_p(N^{-2\delta}). \quad (\text{B.18})$$

By virtue of (B.15) and (B.18), we prove that

$$\sup_{h \leq \tau \leq T-h} \sum_{j=1}^N \left\| \frac{1}{p} \sum_{s=1}^N \Delta \tilde{F}_s(\tau) \mathbf{R}_{s,1}(\tau)^\top \mathbf{R}_{j,3}(\tau) \right\|^2 = O_P \left(\frac{\bar{\omega}_p \log N}{p} + N^{-2\delta} \right), \quad (\text{B.19})$$

and similarly,

$$\sup_{h \leq \tau \leq T-h} \sum_{j=1}^N \left\| \frac{1}{p} \sum_{s=1}^N \Delta \tilde{F}_s(\tau) \mathbf{R}_{s,3}(\tau)^\top \mathbf{R}_{j,1}(\tau) \right\|^2 = O_P \left(\frac{\bar{\omega}_p \log N}{p} + N^{-2\delta} \right). \quad (\text{B.20})$$

Observe that

$$\begin{aligned} & \sum_{j=1}^N \left\| \frac{1}{p} \sum_{s=1}^N \Delta \tilde{F}_s(\tau) \mathbf{R}_{s,3}(\tau)^\top \mathbf{R}_{j,3}(\tau) \right\|^2 \\ & \leq 2 \sum_{j=1}^N \left\| \sum_{s=1}^N \Delta \tilde{F}_s(\tau) \left[\frac{\mathbf{u}_s^\top \mathbf{u}_j}{p} - \mathbb{E} \left(\frac{\mathbf{u}_s^\top \mathbf{u}_j}{p} \right) \right] \mathbf{K}_h^{1/2}(\mathbf{t}_s - \tau) \right\|^2 \mathbf{K}_h(\mathbf{t}_j - \tau) + \\ & \quad 2 \sum_{j=1}^N \left\| \sum_{s=1}^N \Delta \tilde{F}_s(\tau) \mathbb{E} \left(\frac{\mathbf{u}_s^\top \mathbf{u}_j}{p} \right) \mathbf{K}_h^{1/2}(\mathbf{t}_s - \tau) \right\|^2 \mathbf{K}_h(\mathbf{t}_j - \tau) \\ & \leq 2 \left[\sum_{s=1}^N \left\| \Delta \tilde{F}_s(\tau) \right\|^2 \right] \left[\sum_{s=1}^N \mathbf{K}_h^2(\mathbf{t}_s - \tau) \right] \left[\sum_{s=1}^N \sum_{j=1}^N \left| \frac{\mathbf{u}_s^\top \mathbf{u}_j}{p} - \mathbb{E} \left(\frac{\mathbf{u}_s^\top \mathbf{u}_j}{p} \right) \right|^4 \right]^{1/2} + \\ & \quad 2 \left[\sum_{s=1}^N \left\| \Delta \tilde{F}_s(\tau) \right\|^2 \right] \left[\sum_{s=1}^N \sum_{j=1}^N \left| \mathbb{E} \left(\frac{\mathbf{u}_s^\top \mathbf{u}_j}{p} \right) \right|^2 \mathbf{K}_h(\mathbf{t}_s - \tau) \mathbf{K}_h(\mathbf{t}_j - \tau) \right]. \end{aligned}$$

By Assumption 1(ii), we may show that

$$\begin{aligned} & \sup_{h \leq \tau \leq T-h} \sum_{s=1}^N \sum_{j=1}^N \left| \mathbb{E} \left(\frac{\mathbf{u}_s^\top \mathbf{u}_j}{p} \right) \right|^2 \mathbf{K}_h(\mathbf{t}_s - \tau) \mathbf{K}_h(\mathbf{t}_j - \tau) \\ & = \sup_{h \leq \tau \leq T-h} \sum_{s=1}^N \left| \mathbb{E} \left(\frac{\mathbf{u}_s^\top \mathbf{u}_s}{p} \right) \right|^2 \mathbf{K}_h^2(\mathbf{t}_s - \tau) = O \left(\frac{1}{N h} \right), \end{aligned}$$

which, together with (B.8), leads to

$$\sup_{h \leq \tau \leq T-h} \left[\sum_{s=1}^n \left\| \Delta \tilde{F}_s(\tau) \right\|^2 \right] \left[\sum_{s=1}^N \sum_{j=1}^N \left| \mathbb{E} \left(\frac{\mathbf{u}_s^\top \mathbf{u}_j}{p} \right) \right|^2 \mathbf{K}_h(\mathbf{t}_s - \tau) \mathbf{K}_h(\mathbf{t}_j - \tau) \right] = O_P \left(\frac{1}{N h} \right). \quad (\text{B.21})$$

As in the proof of (B.11) in Kong (2018), by the uniform sparsity assumption (2.6), we have

$$\sum_{s=1}^N \sum_{j=1}^N \mathbb{E} \left[\left| \frac{\mathbf{u}_s^\top \mathbf{u}_j}{p} - \mathbb{E} \left(\frac{\mathbf{u}_s^\top \mathbf{u}_j}{p} \right) \right|^4 \right] = O \left(\left(\frac{\bar{\omega}_p}{Np} \right)^2 \right),$$

which, together with (B.8) and $\frac{1}{N} \sum_{s=1}^N K_h^2(t_j - \tau) = O(h^{-1})$ uniformly over $h \leq \tau \leq T - h$, indicates that

$$\sup_{h \leq \tau \leq T-h} \left[\sum_{s=1}^N \left\| \Delta \tilde{F}_s(\tau) \right\|^2 \right] \left[\sum_{s=1}^N K_h^2(t_s - \tau) \right] \left[\sum_{s=1}^N \sum_{j=1}^N \left| \frac{\mathbf{u}_s^\top \mathbf{u}_j}{p} - \mathbb{E} \left(\frac{\mathbf{u}_s^\top \mathbf{u}_j}{p} \right) \right|^4 \right]^{1/2} = O_P \left(\frac{\bar{\omega}_p}{ph} \right). \quad (\text{B.22})$$

Then, by (B.21) and (B.22), we can prove that

$$\sup_{h \leq \tau \leq T-h} \sum_{j=1}^N \left\| \frac{1}{p} \sum_{s=1}^N \Delta \tilde{F}_s(\tau) \mathbf{R}_{s,3}(\tau)^\top \mathbf{R}_{j,3}(\tau) \right\|^2 = O_P \left(\frac{\bar{\omega}_p}{ph} + \frac{1}{Nh} \right). \quad (\text{B.23})$$

By (3.12), (B.8) and Proposition A.1 in Bu et al. (2023), we can prove that

$$\sup_{h \leq \tau \leq T-h} \sum_{j=1}^N \left\| \frac{1}{p} \sum_{s=1}^N \Delta \tilde{F}_s(\tau) \left[\Delta \tilde{X}_s(\tau) - \Delta X_s(\tau) \right]^\top \Delta X_j(\tau) \right\|^2 = O_P \left(\zeta_1^2(p, b, \mathbf{n}, N) \right) \quad (\text{B.24})$$

and

$$\sup_{h \leq \tau \leq T-h} \sum_{j=1}^N \left\| \frac{1}{p} \sum_{s=1}^N \Delta \tilde{F}_s(\tau) \Delta \tilde{X}_s(\tau)^\top \left[\Delta \tilde{X}_j(\tau) - \Delta X_j(\tau) \right] \right\|^2 = O_P \left(\zeta_1^2(p, b, \mathbf{n}, N) \right). \quad (\text{B.25})$$

By virtue of (B.6), (B.9), (B.10), (B.19), (B.20), (B.23)–(B.25), Assumption 4(ii) and (B.26) in Lemma B.3 below, we complete the proof of (B.2). \blacksquare

Let $V_0(\tau) = \text{diag}\{v_1(\tau), \dots, v_k(\tau)\}$ with $v_j(\tau)$ being the j -th largest eigenvalue of $\Sigma_\Lambda(\tau)$ defined in (3.3), and $\Delta X(\tau)$ be defined similarly to $\Delta \tilde{X}(\tau)$ with $\Delta \tilde{X}_i$ replaced by ΔX_i . Let $W_0(\tau)$ be a $k \times k$ matrix consisting of the eigenvectors of $\Sigma_\Lambda(\tau)$. Lemma B.3 below derives the uniform consistency properties of $\tilde{V}(\tau)$ and $H(\tau)$ both of which are defined above Lemma B.2.

Lemma B.3. *Suppose that Assumptions 1–3 and 4(i)(ii) are satisfied. Then we have*

$$\sup_{h \leq \tau \leq T-h} \left\| \tilde{V}(\tau) - V_0(\tau) \right\|_s = o_P(1) \quad (\text{B.26})$$

and

$$\sup_{h \leq \tau \leq T-h} \|H(\tau) - H_0(\tau)\|_s = o_P(1), \quad (\text{B.27})$$

where $H_0(\tau) = [V_0(\tau)]^{-1/2} W_0(\tau) [\Sigma_\Lambda(\tau)]^{1/2}$.

Proof of Lemma B.3. We start with the proof of (B.26). By Weyl's inequality, we have

$$\begin{aligned} & \sup_{h \leq \tau \leq T-h} \max_{1 \leq l \leq k} |\tilde{v}_l(\tau) - v_l(\tau)| \\ & \leq \sup_{h \leq \tau \leq T-h} \left\| \frac{1}{p} \Delta \tilde{X}(\tau)^\top \Delta \tilde{X}(\tau) - \frac{1}{p} \Delta X(\tau)^\top \Delta X(\tau) \right\|_s + \\ & \quad \sup_{h \leq \tau \leq T-h} \left\| \frac{1}{p} \Delta X(\tau)^\top \Delta X(\tau) - \Delta F(\tau) \left[\frac{1}{p} \Lambda(\tau)^\top \Lambda(\tau) \right] \Delta F(\tau)^\top \right\|_s + \\ & \quad \sup_{h \leq \tau \leq T-h} \left\| \frac{1}{p} \Lambda(\tau) [\Delta F(\tau)^\top \Delta F(\tau) - I_k] \Lambda(\tau)^\top \right\|_s + \\ & \quad \sup_{h \leq \tau \leq T-h} \left\| \frac{1}{p} \Lambda(\tau)^\top \Lambda(\tau) - \Sigma_\Lambda(\tau) \right\|_s. \end{aligned} \quad (\text{B.28})$$

By (3.12) in Remark 3.2 and (3.7) in Assumption 4(ii), we may show that

$$\begin{aligned} & \sup_{h \leq \tau \leq T-h} \left\| \frac{1}{p} \Delta \tilde{X}(\tau)^\top \Delta \tilde{X}(\tau) - \frac{1}{p} \Delta X(\tau)^\top \Delta X(\tau) \right\|_s \\ & \leq \sup_{h \leq \tau \leq T-h} \left\| \frac{1}{p} [\Delta \tilde{X}(\tau) - \Delta X(\tau)]^\top \Delta \tilde{X}(\tau) \right\|_s + \\ & \quad \sup_{h \leq \tau \leq T-h} \left\| \frac{1}{p} \Delta X(\tau)^\top [\Delta \tilde{X}(\tau) - \Delta X(\tau)] \right\|_s \\ & = O_P(\zeta_1(p, b, \mathbf{n}, N)) = o_P(1), \end{aligned} \quad (\text{B.29})$$

where $\zeta_1(p, b, \mathbf{n}, N)$ is defined in Assumption 4(iii). Using Proposition A.1 in [Bu et al. \(2023\)](#) and noting that $\sigma_t^F = I_k$, we have

$$\sup_{h \leq \tau \leq T-h} \|\Delta F(\tau)^\top \Delta F(\tau) - I_k\|_s = o_P(1),$$

which, together with (3.10), indicates that

$$\sup_{h \leq \tau \leq T-h} \left\| \frac{1}{p} \Lambda(\tau) [\Delta F(\tau)^\top \Delta F(\tau) - I_k] \Lambda(\tau)^\top \right\|_s = o_P(1). \quad (\text{B.30})$$

By (3.3) in Assumption 1(iii), we readily have that

$$\sup_{h \leq \tau \leq T-h} \left\| \frac{1}{p} \Lambda(\tau)^\top \Lambda(\tau) - \Sigma_\Lambda(\tau) \right\|_s = o_p(1). \quad (\text{B.31})$$

By (B.28)–(B.31), to complete the proof of (B.26), it remains to show that

$$\sup_{h \leq \tau \leq T-h} \left\| \frac{1}{p} \Delta X(\tau)^\top \Delta X(\tau) - \Delta F(\tau) \left[\frac{1}{p} \Lambda(\tau)^\top \Lambda(\tau) \right] \Delta F(\tau)^\top \right\|_s = o_p(1). \quad (\text{B.32})$$

Letting $\Delta X_{i,s}(\tau)$ be the i -th element of $\Delta X_s(\tau)$ and $\sigma_{i,\bullet,t}^u$ the i -th row vector of σ_t^u , it follows from (1.2) and (2.4) that

$$\begin{aligned} \Delta X_{i,s}(\tau) &= \left\{ \left(\int_{t_{s-1}}^{t_s} \Lambda_i(t)^\top dF_t \right) + \left(\int_{t_{s-1}}^{t_s} \mu_{i,t}^u dt \right) + \left[\int_{t_{s-1}}^{t_s} (\sigma_{i,\bullet,t}^u)^\top dW_t^u \right] \right\} K_h^{1/2}(t_s - \tau) \\ &=: R_{i,s,1}(\tau) + R_{i,s,2}(\tau) + R_{i,s,3}(\tau). \end{aligned}$$

Then we write

$$R_{i,\bullet,l}(\tau) = [R_{i,1,l}(\tau), \dots, R_{i,n,l}(\tau)]^\top, \quad i = 1, \dots, p, \quad l = 1, 2, 3,$$

and

$$\frac{1}{p} \Delta X(\tau)^\top \Delta X(\tau) = \sum_{l_1=1}^3 \sum_{l_2=1}^3 \frac{1}{p} \sum_{i=1}^p R_{i,\bullet,l_1}(\tau) R_{i,\bullet,l_2}(\tau)^\top.$$

Similarly to the proofs of (B.6), (B.9), (B.19) and (B.23), we may show that uniformly over $h \leq \tau \leq T - h$,

$$\left\| \frac{1}{p} \sum_{i=1}^p R_{i,\bullet,1}(\tau) R_{i,\bullet,1}(\tau)^\top - \Delta F(\tau) \left[\frac{1}{p} \Lambda(\tau)^\top \Lambda(\tau) \right] \Delta F(\tau)^\top \right\|_s = O_p(h^\delta \log(p \vee N)), \quad (\text{B.33})$$

$$\frac{1}{p} \left\| \sum_{i=1}^p \sum_{l=1}^3 R_{i,\bullet,2}(\tau) R_{i,\bullet,l}(\tau)^\top + \sum_{i=1}^p \sum_{l=1}^3 R_{i,\bullet,l}(\tau) R_{i,\bullet,2}(\tau)^\top \right\|_s = O_p \left(\sqrt{\frac{\log(p \vee N)}{N}} \right), \quad (\text{B.34})$$

$$\frac{1}{p} \left\| \sum_{i=1}^p R_{i,\bullet,1}(\tau) R_{i,\bullet,3}(\tau)^\top + \sum_{i=1}^p R_{i,\bullet,3}(\tau) R_{i,\bullet,1}(\tau)^\top \right\|_s = O_p \left(\sqrt{\frac{\omega_p \log^2(p \vee N)}{ph}} + \sqrt{\frac{\log(p \vee N)}{N^{2\delta}}} \right) \quad (\text{B.35})$$

$$\frac{1}{p} \left\| \sum_{i=1}^p R_{i,\bullet,3}(\tau) R_{i,\bullet,3}(\tau)^\top \right\|_s = O_p \left(\sqrt{\frac{\omega_p}{ph}} + \frac{1}{Nh} \right). \quad (\text{B.36})$$

Combining (B.33)–(B.36) with Assumption 4(ii)(iii), we complete the proof of (B.26).

We next turn to the proof of (B.27) which is similar to the proof of (A.10) in Kong (2018). Let

$\widetilde{W}(\tau) = W(\tau)[Q(\tau)]^{-1}$, where

$$W(\tau) = \left[\frac{1}{p} \Lambda(\tau)^\top \Lambda(\tau) \right]^{1/2} \left[\Delta F(\tau)^\top \Delta \widetilde{F}(\tau) \right], \quad Q(\tau) = [\text{diag} \{W(\tau)^\top W(\tau)\}]^{1/2}.$$

Define

$$\begin{aligned} M(\tau) &= \left[\frac{1}{p} \Lambda(\tau)^\top \Lambda(\tau) \right]^{1/2} [\Delta F(\tau)^\top \Delta F(\tau)] \left[\frac{1}{p} \Lambda(\tau)^\top \Lambda(\tau) \right]^{1/2}, \\ D(\tau) &= \left[\frac{1}{p} \Lambda(\tau)^\top \Lambda(\tau) \right]^{1/2} \Delta F(\tau)^\top \left[\frac{\Delta \widetilde{X}(\tau)^\top \Delta \widetilde{X}(\tau) - \Delta F(\tau) \Lambda(\tau)^\top \Lambda(\tau) \Delta F(\tau)^\top}{p} \right] \Delta \widetilde{F}(\tau). \end{aligned}$$

By the definition of $\Delta \widetilde{F}(\tau)$ in (B.3), we have

$$\{M(\tau) + D(\tau)[W(\tau)]^{-1}\} \widetilde{W}(\tau) = \widetilde{W}(\tau) \widetilde{V}(\tau),$$

indicating that $\widetilde{W}(\tau)$ is a $k \times k$ matrix consisting of the eigenvectors of $M(\tau) + D(\tau)[W(\tau)]^{-1}$. Write

$$H(\tau) = [\widetilde{V}(\tau)]^{-1} [Q(\tau) \widetilde{W}(\tau)^\top] \left[\frac{1}{p} \Lambda(\tau)^\top \Lambda(\tau) \right]^{1/2}.$$

Hence, in order to prove (B.27), we only need to show

$$\sup_{h \leq \tau \leq T-h} \|Q^2(\tau) - V_0(\tau)\|_s = o_P(1), \quad (\text{B.37})$$

$$\sup_{h \leq \tau \leq T-h} \|\widetilde{W}(\tau) - W_0(\tau)\|_s = o_P(1). \quad (\text{B.38})$$

Let $W_*(\tau)$ be a $k \times k$ matrix consisting of the eigenvectors of $M(\tau)$. By the $\sin \theta$ theorem in Davis and Kahan (1970), we have

$$\|\widetilde{W}(\tau) - W_0(\tau)\|_s \leq C \|D(\tau)\|_s \cdot \|[W(\tau)]^{-1}\|_s. \quad (\text{B.39})$$

Using (3.3) in Assumption 1(iii) and Lemma B.2, and noting that $H(\tau)$ is asymptotically non-singular, we may show that

$$\sup_{h \leq \tau \leq T-h} \|[W(\tau)]^{-1}\|_s = O_P(1). \quad (\text{B.40})$$

Meanwhile, by (3.3), (B.8), (B.12), (B.29) and (B.32), we can prove that

$$\sup_{h \leq \tau \leq T-h} \|D(\tau)\|_s$$

$$\begin{aligned}
&\leq C \sup_{h \leq \tau \leq T-h} \left\| \frac{\Delta \tilde{X}(\tau)^\top \Delta \tilde{X}(\tau) - \Delta F(\tau) \Lambda(\tau)^\top \Lambda(\tau) \Delta F(\tau)^\top}{p} \right\|_s \\
&\leq C \sup_{h \leq \tau \leq T-h} \left\| \frac{\Delta X(\tau)^\top \Delta X(\tau) - \Delta F(\tau) \Lambda(\tau)^\top \Lambda(\tau) \Delta F(\tau)^\top}{p} \right\|_s + o_P(1) \\
&= o_P(1).
\end{aligned} \tag{B.41}$$

By virtue of (B.39)–(B.41), we complete the proof of (B.38).

It remains to prove (B.37). By the triangular inequality, we have

$$\|Q^2(\tau) - V_0(\tau)\|_s \leq \|Q^2(\tau) - \tilde{V}(\tau)\|_s + \|\tilde{V}(\tau) - V_0(\tau)\|_s.$$

By (B.3), (B.29) and (B.32),

$$\begin{aligned}
&\sup_{h \leq \tau \leq T-h} \|Q^2(\tau) - \tilde{V}(\tau)\|_s \\
&\leq C \sup_{h \leq \tau \leq T-h} \left\| \Delta \tilde{F}(\tau)^\top \frac{\Delta \tilde{X}(\tau)^\top \Delta \tilde{X}(\tau) - \Delta F(\tau) \Lambda(\tau)^\top \Lambda(\tau) \Delta F(\tau)^\top}{p} \Delta \tilde{F}(\tau) \right\|_s \\
&\leq C \sup_{h \leq \tau \leq T-h} \left\| \frac{\Delta X(\tau)^\top \Delta X(\tau) - \Delta F(\tau) \Lambda(\tau)^\top \Lambda(\tau) \Delta F(\tau)^\top}{p} \right\|_s + o_P(1) \\
&= o_P(1).
\end{aligned} \tag{B.42}$$

Then, by (B.26) and (B.42), we complete the proof of (B.37). \blacksquare

Let $H_*(\tau) = [H(\tau)]^{-1}$ be the inverse of the rotation matrix $H(\tau)$. The following lemma derives the uniform convergence rate for the estimated factor loading functions.

Lemma B.4. *Suppose that Assumptions 1–3 and 4(i)(ii) are satisfied. Then,*

$$\max_{1 \leq i \leq p} \sup_{h \leq \tau \leq T-h} \left\| \tilde{\Lambda}_i(\tau) - H_*(\tau)^\top \Lambda_i(\tau) \right\| = O_P(\zeta_1(p, b, \mathbf{n}, N) + \zeta_2(p, h, N)) \tag{B.43}$$

where $\zeta_1(p, b, \mathbf{n}, N)$ and $\zeta_2(p, h, N)$ are defined in Assumption 4(iii) and $H_*(\tau) = H(\tau)^\top + o_P(1)$ uniformly over $h \leq \tau \leq T-h$.

Proof of Lemma B.4. By (1.2) and the definition of $\tilde{\Lambda}_i(\tau)$, we have

$$\begin{aligned}
\tilde{\Lambda}_i(\tau) &= \sum_{j=1}^N \Delta \tilde{X}_{i,j} \Delta \tilde{F}_j(\tau) K_h^{1/2}(t_j - \tau) \\
&= \sum_{j=1}^N \left[\int_{t_{j-1}}^{t_j} \Lambda_i(t)^\top F_t dt \right] H(\tau) \Delta F_j(\tau) K_h^{1/2}(t_j - \tau) + \sum_{j=1}^N \Delta U_{i,j}(\tau) H(\tau) \Delta F_j(\tau) +
\end{aligned}$$

$$\begin{aligned} & \sum_{j=1}^N \Delta X_{i,j} \left[\Delta \tilde{F}_j(\tau) - H(\tau) \Delta F_j(\tau) \right] K_h^{1/2}(t_j - \tau) + \\ & \sum_{j=1}^N \left(\Delta \tilde{X}_{i,j} - \Delta X_{i,j} \right) \Delta \tilde{F}_j(\tau) K_h^{1/2}(t_j - \tau), \end{aligned}$$

where $\Delta U_{i,j}(\tau) = (U_{i,t_j} - U_{i,t_{j-1}}) K_h^{1/2}(t_j - \tau)$.

Using (3.12), (B.8) and the Cauchy-Schwarz inequality, we may show that

$$\begin{aligned} & \max_{1 \leq i \leq p} \sup_{h \leq \tau \leq T-h} \left\| \sum_{j=1}^N \left(\Delta \tilde{X}_{i,j} - \Delta X_{i,j} \right) \Delta \tilde{F}_j(\tau) K_h^{1/2}(t_j - \tau) \right\| \\ & \leq \max_{1 \leq i \leq p} \sup_{h \leq \tau \leq T-h} \left[\sum_{j=1}^N \left(\Delta \tilde{X}_{i,j} - \Delta X_{i,j} \right)^2 K_h(t_j - \tau) \right]^{1/2} \sup_{h \leq \tau \leq T-h} \left[\sum_{s=1}^N \left\| \Delta \tilde{F}_s(\tau) \right\|^2 \right]^{1/2} \\ & = O_P(\zeta_1(p, b, \mathbf{n}, N)) \cdot O_P(1) = O_P(\zeta_1(p, b, \mathbf{n}, N)). \end{aligned} \quad (\text{B.44})$$

By Lemma B.2, we have

$$\begin{aligned} & \max_{1 \leq i \leq p} \sup_{h \leq \tau \leq T-h} \left\| \sum_{j=1}^N \Delta X_{i,j} \left[\Delta \tilde{F}_j(\tau) - H(\tau) \Delta F_j(\tau) \right] K_h^{1/2}(t_j - \tau) \right\| \\ & = O_P(\zeta_1(p, b, \mathbf{n}, N) + \zeta_2(p, h, N)). \end{aligned} \quad (\text{B.45})$$

Following the proof of Proposition A.1 in Bu *et al.* (2023), we can prove that

$$\max_{1 \leq i \leq p} \sup_{h \leq \tau \leq T-h} \left\| \sum_{j=1}^N \Delta U_{i,j}(\tau) \Delta F_j(\tau) \right\| = O_P \left(\sqrt{\frac{\log(p \vee N)}{Nh}} \right),$$

which, together with the fact that $\sup_{h \leq \tau \leq T-h} \|H(\tau)\|_s = O_P(1)$ by Lemma B.3, leads to

$$\begin{aligned} & \max_{1 \leq i \leq p} \sup_{h \leq \tau \leq T-h} \left\| \sum_{j=1}^N \Delta U_{i,j}(\tau) H(\tau) \Delta F_j(\tau) \right\| \\ & = O_P \left(\sqrt{\frac{\log(p \vee N)}{Nh}} \right) = O_P(\zeta_2(p, h, N)). \end{aligned} \quad (\text{B.46})$$

By (B.44)–(B.46) and noting that $\zeta_2^\circ(p, h, N) = O(\zeta_2(p, h, N))$, we only need to show that

$$\max_{1 \leq i \leq p} \sup_{h \leq \tau \leq T-h} \left\| \sum_{j=1}^N \left[\int_{t_{j-1}}^{t_j} \Lambda_i(t)^\top F_t dt \right] H(\tau) \Delta F_j(\tau) K_h^{1/2}(t_j - \tau) - H_*(\tau)^\top \Lambda_i(\tau) \right\|$$

$$= O_P(\zeta_1(p, b, \mathbf{n}, N) + \zeta_2(p, h, N)). \quad (\text{B.47})$$

By (B.12), (B.27) and the smoothness condition in Assumption 1(iii), we have

$$\max_{1 \leq i \leq p} \sup_{h \leq \tau \leq T-h} \left\| \sum_{j=1}^N \left[\int_{t_{j-1}}^{t_j} \Lambda_i(t)^\top F_t dt \right] H(\tau) \Delta F_j(\tau) K_h^{1/2}(t_j - \tau) - H(\tau) \Delta F(\tau)^\top \Delta F(\tau) \Lambda_i(\tau) \right\| = O_P(h^\delta). \quad (\text{B.48})$$

On the other hand, by Lemmas B.2 and B.3 as well as Assumption 1(iii), we have

$$\begin{aligned} & H(\tau) \Delta F(\tau)^\top \Delta F(\tau) \Lambda_i(\tau) - H_*(\tau)^\top \Lambda_i(\tau) \\ &= \left[H(\tau) \Delta F(\tau)^\top \Delta F(\tau) H(\tau)^\top - \tilde{\Delta F}(\tau)^\top \tilde{\Delta F}(\tau) \right] H_*(\tau)^\top \Lambda_i(\tau) \\ &\leq C \left\| \Delta F(\tau) H(\tau)^\top - \tilde{\Delta F}(\tau) \right\| \\ &= O_P(\zeta_1(p, b, \mathbf{n}, N) + \zeta_2^\circ(p, h, N)). \end{aligned} \quad (\text{B.49})$$

By virtue of (B.48) and (B.49), we prove (B.47), thus completing the proof of (B.43).

Finally, by (B.27) in Lemma B.3, we readily have that

$$\sup_{h \leq \tau \leq T-h} \left\| H(\tau) H(\tau)^\top - I_k \right\|_s = o_P(1),$$

indicating that $H_*(\tau) = H(\tau)^\top + o_P(1)$ uniformly over $h \leq \tau \leq T - h$. ■

References

- BOSQ, D. (1998). *Nonparametric Statistics for Stochastic Processes: Estimation and Prediction*. Springer.
- BU, R., LI, D., LINTON, O. AND WANG, H. (2023). Nonparametric estimation of large spot volatility matrices for high-frequency financial data. Working paper available at <https://arxiv.org/abs/2307.01348>.
- DAVIS, C. AND KAHAN, W. M. (1970). The rotation of eigenvectors by a perturbation. III. *SIAM Journal on Numerical Analysis* **7**, 1–46.
- FAN, J., FAN, Y. AND LV, J. (2008). High dimensional covariance matrix estimation using a factor model. *Journal of Econometrics* **147**, 186–197.
- FAN, J., LIAO, Y. AND MINCHEVA, M. (2013). Large covariance estimation by thresholding principal orthogonal complements (with discussion). *Journal of the Royal Statistical Society, Series B* **75**, 603–680.
- KONG, X. (2018). On the systematic and idiosyncratic volatility with large panel high-frequency data. *Annals of Statistics* **46**, 1077–1108.